Figure 2. MS/MS spectrum of fucosylated biantennary *N*-linked oligosaccharide (peak M1) detected in the insoluble fraction from CHO-III.
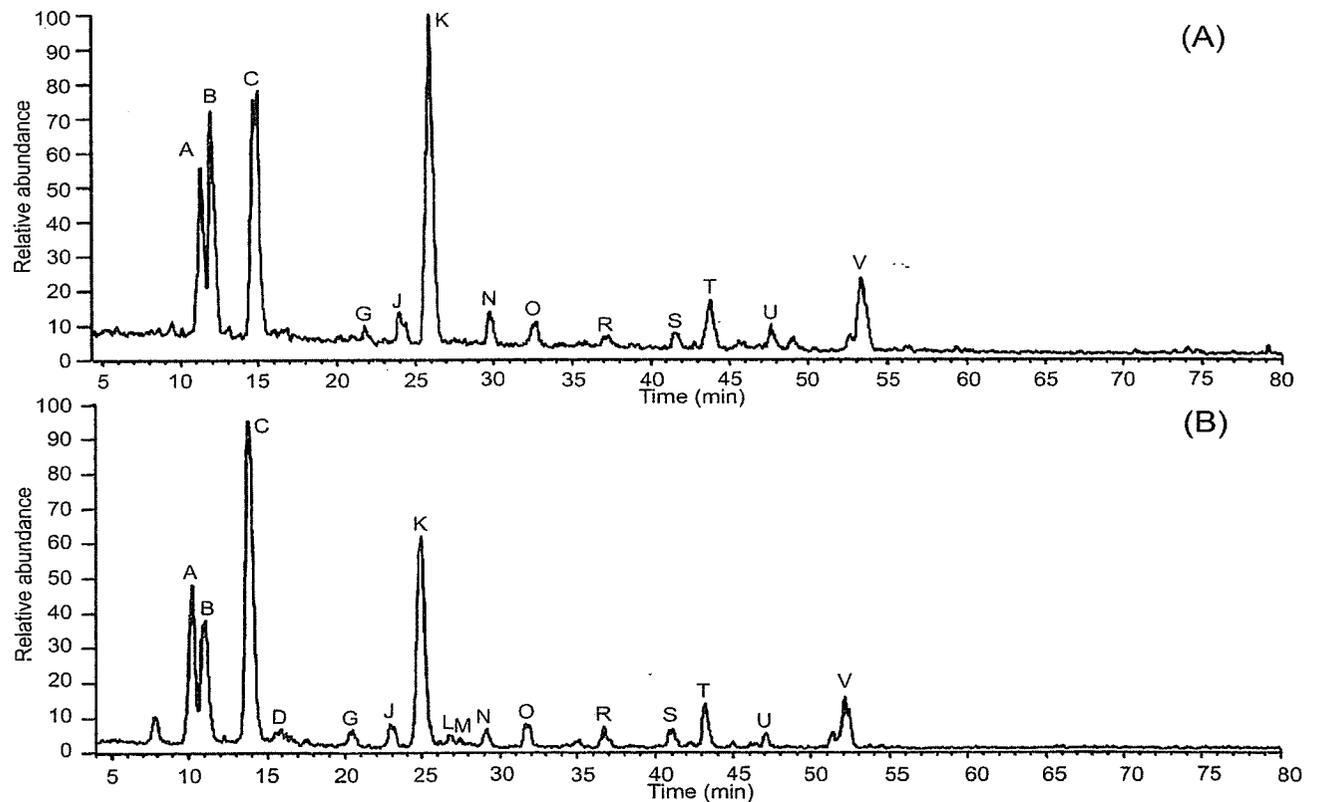

Figure 3. Total ion chromatograms of GCC-LC/MS of borohydride-reduced *N*-linked oligosaccharides released from the soluble fractions of CHO (A) and CHO-III (B) in positive ion mode. Pump A: 5 mM ammonium acetate, pH 8.5, containing 2% ACN. Pump B: 5 mM ammonium acetate, pH 8.5, containing 80% ACN. The borohydride-reduced oligosaccharides were eluted at a flow rate of 2 μL/min with a gradient of 10–45% of pump B in 90 min.

3.3 Identification of protein bearing bisected oligosaccharides

To identify proteins with altered glycans by the expression of GnT-III, we performed 2-DE followed by lectin blotting using PHA-E4 lectin, which recognizes bisecting GlcNAc in complex-type oligosaccharides. Although some bisected glycoproteins (70–120 kDa) could be visualized by 2-D lectin blotting, their expressions were too low to be detected on 2-DE gel. Lectin affinity chromatography, which is generally used for the concentration of glycoproteins, cannot be used for the insoluble fraction due to the presence of detergent in the solvent medium. Therefore, we first performed 1-D SDS-PAGE followed by lectin blotting, and then proteins in the range of 70–120 kDa were extracted from the gel (Fig. 4). 2-DE followed by lectin blotting was then performed, and interesting spots were successfully detected on 2-DE gel. Figure 5A and B shows the 2-DE gel images and the 2-D lectin blot of extracted proteins, respectively. The remarkable train spots (120 Da) of glycoprotein were picked up and in-gel digested with trypsin. The digest was subjected to LC/MS/MS, and the integrin α3 precursor was identified as the GnT-III target protein.

4 Discussion

The development of a simple and rapid method to explore glycan structural alteration in a complex mixture is required to elucidate the mechanisms of diseases involving glycan alteration. In this study, we demonstrated that GCC-LC/MS, which is used for glycosylation analysis in glycoproteins, is
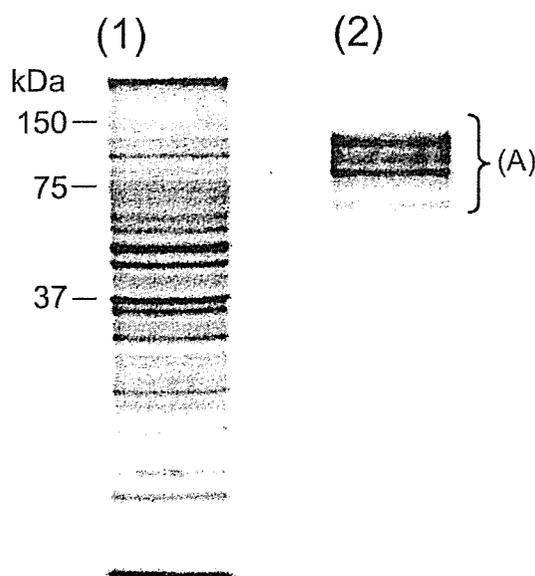

Figure 5. Enlarged partial (A) 2-DE and (B) lectin blot images from band A in Fig. 4.

applicable for the exploration of changes in glycosylation between samples. Using GCC-LC/MS, high mannose, hybrid, and complex types as well as neutral and acidic oligosaccharides could be separated and characterized by a single analysis. GCC-LC/MS clearly shows differences in glycosylation between soluble and insoluble fractions. High mannose-type oligosaccharides were detected as major components in the soluble fraction. The soluble fraction contains endoplasmic reticulum and Golgi apparatus, where N-linked oligosaccharides are constructed. The predominance of high-mannose-type oligosaccharides in the soluble fraction may be the cause of immature oligosaccharides in the process of biosynthesis. In contrast, complex and hybrid types with or without sialic acids were detected in the insoluble fraction, suggesting that membrane proteins carry mature oligosaccharides.

In addition, GCC-LC/MS revealed differences in glycosylation between control cells and aberrant model cells. Biantennary forms bearing extra GlcNAc were obviously increased in cells transfected with the GnT-III gene, indicating that our methodology allows us to explore changes in the glycosyltransferase expression followed by glycan alteration. Although MS is frequently used for the analysis of glycosylation, identification of oligosaccharide isomers by MS alone

Figure 4. (1) 1-D SDS-PAGE and (2) lectin blot images of the CHO-III insoluble fraction. Proteins were separated on a 12.5% SDS-PAGE gel and stained with SYPRO Orange.
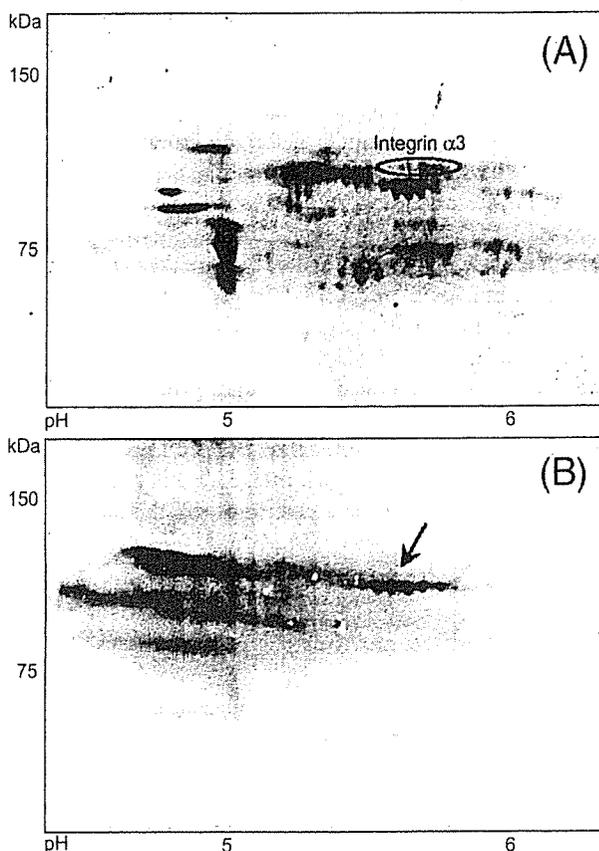
still remains challenges. Positional isomers could be differentiated by multiple-stage tandem mass spectrometry (MS^n); however, MS^n itself failed to identify oligosaccharides if the sample contained positional isomers. The use of GCC-LC/MS enables us to differentiate the structural isomers and perform differential analysis in glycosylation between normal and aberrant cells.

GnT-III is reported to involve the suppression of tumor cell metastasis and is assumed to be a marker of cancerous alteration in hepatic carcinoma [21, 22]. To identify the protein in which glycosylation was modified by GnT-III expression, we carried out 2-DE followed by lectin blotting, and Integrin α3 was identified as a target protein of GnT-III. Integrin α3, a type I membrane protein, is known to be a receptor of adhesion molecules, such as laminin 5 and 10/11 [23–25]. Our finding, in which integrin α3 is a target molecule of GnT-III, might be a clue to clarify the suppression mechanism of metastasis by GnT-III.

5 Concluding remarks

We propose a strategy for glycomic/glycoproteomic analysis using GCC-LC/MS in Fig. 6. First, GCC-LC/MS is used for oligosaccharide profiling to identify disease-related oligosaccharides. Based on the carbohydrate structure, appropriate lectins or antibodies could be selected for western blotting. Proteins carrying disease-related oligosaccharides could then be identified by 2-D lectin blotting followed by MS/MS analysis. Using several groups, 2-D lectin blotting has been proposed for the characterization of glycoproteins on gel [26, 27]. The use of mass spectrometric oligosaccharide profiling, which can directly characterize glycan structures, is worthwhile to obtain structural information about disease-related carbohydrate and is helpful in the subsequent choice of appropriate lectins and antibodies. Our method is expected to be a powerful tool for glycomic/glycoproteomic analysis.
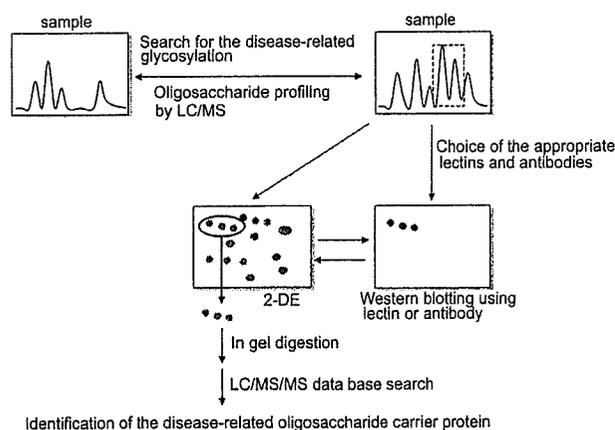

Figure 6. Strategy for glycomics/glycoproteomics using GCC-LC/MS, 2-DE and 2-D Western blotting using lectin or antibody.

6 References

[1] Varki, A., *Glycobiology* 1993, *3*, 97–130.

[2] Isaji, T., Gu, J., Nishiuchi, R., Zhao, Y. *et al.*, *J. Biol. Chem.* 2004, *279*, 19747–19754.

[3] Stanley, P., *Biochim. Biophys. Acta* 2002, *1573*, 363–368.

[4] Schachter, H., *Cell Mol. Life Sci.* 2001, *58*, 1085–1104.

[5] Dennis, J. W., Granovsky, M., Warren, C.E., *Biochim. Biophys. Acta* 1999, *1473*, 21–34.

[6] Delves, P. J., *Autoimmunity* 1998, *27*, 239–253.

[7] Gleeson, P. A., *Biochim. Biophys. Acta* 1994, *1197*, 237–255.

[8] Chui, D., Sellakumar, G., Green, R., Sutton-Smith, M. *et al.*, *Proc. Natl. Acad. Sci. USA* 2001, *98*, 1142–1147.

[9] Itoh, S., Kawasaki, N., Ohta, M., Hyuga, M. *et al.*, *J. Chromatogr. A* 2002, *968*, 89–100.

[10] Kawasaki, N., Haishima, Y., Ohta, M., Itoh, S. *et al.*, *Glycobiology* 2001, *11*, 1043–1049.

[11] Kawasaki, N., Ohta, M., Itoh, S., Hyuga, M. *et al.*, *Biologicals* 2002, *30*, 113–123.

[12] Davies, M., Smith, K. D., Harbin, A. M., Hounsell, E. F., *J. Chromatogr.* 1992, *609*, 125–131.

[13] Narasimhan, S., *J. Biol. Chem.* 1982, *257*, 10235–10242.

[14] Yoshimura, M., Ihara, Y., Matsuzawa, Y., Taniguchi, N., *J. Biol. Chem.* 1996, *271*, 13811–13815.

[15] Taniguchi, N., Miyoshi, E., Ko, J. H., Ikeda, Y., Ihara, Y., *Biochim. Biophys. Acta* 1999, *1455*, 287–300.

[16] Yoshimura, M., Nishikawa, A., Ihara, Y., Taniguchi, S., Taniguchi, N., *Proc. Natl. Acad. Sci. USA.* 1995, *92*, 8754–8758.

[17] Bhaumik, M., Harris, T., Sundaram, S., Johnson, L. *et al.*, *Cancer Res.* 1998, *58*, 2881–2887.

[18] Laemmli, U. K., *Nature* 1970, *227*, 680–685.

[19] Stanley, S., Sundaram, S., Tang, J., Shi, S., *Glycobiology* 2005, *15*, 43–53.

[20] Lee, J., Sundaram, S., Shaper, N. L., Raju, S., Stanley, P., *J. Biol .Chem.* 2001, *276*, 13924–13934.

[21] Yamashita, K., Koide, N., Endo, T., Iwaki, Y., Kobata, A., *J. Biol. Chem.* 1989, *264*, 2415–2423.

[22] Yamashita, K., Hitoi, A., Taniguchi, N., Yokosawa, N. *et al.*, *Cancer Res.* 1983, *43*, 5059–5063.

[23] Carter, W. G., Ryan, M. C., Gahr, P. J., *Cell* 1991, *65*, 599–610.

[24] Kikkawa, Y., Umeda, M., Miyazaki, K., *J. Biochem (Tokyo)* 1994, *116*, 862–869.

[25] Kikkawa, Y., Sanzen, N., Sekiguchi, K., *J. Biol. Chem.* 1998, *273*, 15854–15859.

[26] Kim, Y. S., Hwang, S. Y., Oh, S., Shon, H. *et al.*, *Proteomics* 2004, *4*, 3353–3358.

[27] Rahman, M. A., Karsani, S. A., Othman, I., Rahman, P. S. A., Hashim, O. H., *Biochem. Biophys. Res. Commun.* 2002, *295*, 1007–1013.

Thrombomodulin Enhances the Invasive Activity of Mouse Mammary Tumor Cells

Shingo Niimi[1,*], Mizuho Harashima[2], Kazuko Takayama[2], Mayumi Hara[2], Masashi Hyuga[1], Taiichiro Seki[2], Toyohiko Ariga[2], Toru Kawanishi[1] and Takao Hayakawa[3]

[1]*Division of Biological Chemistry and Biologicals, National Institute of Health Sciences, Kamiyoga 1-18-1, Setagaya-ku, Tokyo 158-8501;* [2]*Department of Nutrition and Physiology, Nihon University College of Bioresource Sciences, Kameino, Fujisawa 252-8510; and* [3]*Deputy Director General, National Institute of Health Sciences, Kamiyoga 1-18-1, Setagaya-ku, Tokyo 158-8501*

Thrombomodulin (TM) is a thrombin receptor on the surface of endothelial cells that converts thrombin from a procoagulant to an anticoagulant. Thrombin promotes invasion by various tumor cells, and positive or negative correlations are found between the expression of TM and tumorigenesis in some patients. In this study, we used an invasion assay to investigate the effect of TM on the invasive activity of a mouse mammary tumor cell line, MMT cells, and the effects of TM were compared with those of thrombin as a positive control. In the presence of 1% fetal calf serum (FCS), TM significantly stimulated MMT cell invasion in a dose-dependent manner, resulting in an approximately 3-fold increase at 1–10 pg/ml over the untreated control. Thrombin also caused a similar degree of stimulation at 50 ng/ml. Since thrombin activity was detected in the components of the assay system, an invasion assay was also performed in a thrombin-activity-depleted assay system constructed to eliminate the effect of thrombin activity; TM (10 pg/ml) plus thrombin (1 pg/ml) stimulated invasion by approximately 3.5-fold in this assay system. Hirudin, a specific thrombin inhibitor, inhibited stimulation by TM as well as by thrombin in both the presence and absence of 1% FCS. Investigations of the effects of TM on proliferation, adhesion and chemotaxis to clarify the mechanism of stimulation by TM revealed that TM does not affect proliferation or adhesion in the presence of 1% FCS, but stimulates chemotaxis by approximately 2.3-fold. Similar results were obtained in experiments using thrombin. TM (10 pg/ml) plus thrombin (1 pg/ml), on the other hand, stimulated chemotaxis by approximately 2.3-fold in the thrombin-activity-depleted assay system. Binding studies using [^{125}I]-thrombin revealed that the cells have specific saturable binding sites for thrombin. These results show that TM stimulates the invasive activity of MMT cells, probably by acting as a cofactor for the thrombin-stimulated invasion of the cells *via* its receptor and lowering the effective concentration of thrombin. The findings also indicate that the stimulation of invasive activity in the presence of 1% FCS and in the thrombin-activity-depleted assay system may mainly be mediated by the stimulation of chemotaxis.

Key words: invasion, thrombin, thrombomodulin.

Abbreviations: TM, thrombomodulin; MEM, modified Eagle's medium; CS, calf serum; FCS, fetal calf serum; MMP, matrix metalloprotease; ECM, extracellular matrix; Boc-Asp(Obzl)-pro-Arg-MCA, Boc-β-benzyl-Asp-Pro-Arg-4-methyl-coumaryl-7-amide; PBS, phosphate-buffered saline.

Thrombomodulin (TM) is a thrombin receptor on the surface of endothelial cells (*1*) that was first discovered as a cofactor for the thrombin-catalyzed activation of the anticoagulant protein C (*2*). Biologically active soluble forms of TM, which probably represent the products of limited proteolytic cleavage of cell-surface TM, were later detected in human plasma (*3*), suggesting a possible role of the soluble forms *in vivo*. TM also positively or negatively regulates various functions of thrombin as described below. TM stimulates the inactivation of pro-

urokinase-type plasminogen activator (*4*), the activation of TAF I (*5*), and the activation of progelatinase A (*6*). TM inhibits the activation of platelets (*7*), the activation of factor X (*8*) and human endothelial cells (*9*), the stimulation of fibrin formation (*8*), and the proliferation of arterial smooth muscle cells (*10*) and human umbilical vein endothelial cells (*11*).

On the other hand, there are several direct and indirect lines of evidence indicating that thrombin stimulates invasion and/or metastasis by tumor cells (*12–18*), and it has recently been reported that the expression of TM is increased or decreased in some carcinomas. The expression of TM increases in squamous carcinomas of the lung (*19*), colorectal carcinomas (*20*), and some transitional

---

*To whom correspondence should be addressed. Tel: +81-3-3700-9347, Fax: +81-3-3700-9084, E-mail: niimi@nihs.go.jp

carcinomas (21–22), and its expression level is negatively correlated with the malignancy of carcinoma of the esophagus (23), hepatocellular carcinoma (24), and ovarian tumors (25). There is also evidence of increased serum levels of TM in some tumors, including pancreatic cancer (26), digestive tract carcinoma (27), and glioblastoma (28). Based on this evidence, it is likely that TM plays some role in the regulation of tumor metastasis.

In this study, we investigated the effects of TM on the invasive activity of a mouse mammary tumor cell line, MMT, by an in vitro invasion assay, because tumor cell invasion through the basement membrane is a critical step in the process of metastasis (29–30). We also compared the effects of TM with those of thrombin as a positive control.

MATERIALS AND METHODS

Materials—TM was a kind gift of Asahi Kasei Pharma, Japan. The TM was prepared as described by Gomi et al. (31). Plasmids containing the cDNA encoding TM (residues 1–498) were transfected into COS-1 cells, and the recombinant TM was purified from serum-free COS-1-cell-conditioned medium. The purified TM yielded a single band at 90 kDa in SDS-PAGE under reducing conditions. The recombinant TM was confirmed to be thrombin-free by a protein C activating assay developed in our laboratory (32). Thrombin (1,140 units/mg protein) was a kind gift of Mochida Pharmaceutical Co., Ltd., Japan. Hirudin was purchased from Wako (Osaka, Japan). A fluorogenic substrate, Boc-β-benzyl-Asp-Pro-Arg-4-methyl-coumaryl-7-amide (Boc-Asp(Obzl)-pro-Arg-MCA), was purchased from Peptide Institute, Inc. (Osaka, Japan).

Cell Culture—MMT mouse mammary tumor cells were obtained from the Japanese Health Science Research Resource Bank and cultured in modified Eagle's medium (MEM) supplemented with 10% calf serum (CS) on 60-mm diameter culture dishes, 4×10^5 cells per dish. After 7 d, the subconfluent MMT cells were detached from the culture dishes with 0.25% trypsin/EDTA, treated with MEM containing 10% CS, and collected by centrifugation. The cells were then washed with MEM and used in experiments. In some experiments, the thrombin activity associated with cells was depleted as described below, and the resultant cells were used for various experiments in which MEM containing 0.1% BSA was used as the basal medium. We refer to this assay system as the thrombin-activity-depleted assay system below. To deplete thrombin activity, the cell suspension (1.5×10^5 cells in 10 ml of MEM) was incubated in a non-adherent form on 100-mm diameter non-treated culture dishes pre-coated with BSA (10 mg/ml) for 2 h in a humidified chamber at 37°C under 5% CO_2, and then washed with MEM.

In Vitro Invasion Assay—In vitro invasion by MMT cells was measured in a Matrigel invasion chamber (Collaborative Biomedical Products, Bedford, MA, USA). The chamber (upper compartment) was placed in a 24-well culture plate (lower compartment), and the cell suspension (1.6×10^5 cells in 500 µl) and the basal medium (750 µl) containing various factors were added to the upper and lower compartments, respectively. MEM containing 1% fetal calf serum (FCS) or 0.1% BSA was used as the basal medium. Matrigel invasion chambers were pre-coated with fibronectin as described below before use in the thrombin-activity-depleted assay system. Human plasma fibronectin solution (IWAKI, Japan) was diluted to a final concentration of 5 µg/ml with phosphate-buffered saline (PBS), and a 300 µl aliquot was added to the chamber and a 750 µl aliquot to the 24-well culture plate. The chamber and 24-well plate were allowed to stand at 37°C for 2 h and were then washed with PBS. After incubating the cells for 18 h, the filters were fixed with methanol and stained with hematoxylin and eosin. The cells on the upper surface of the filters were removed by wiping with cotton swabs, and the number of cells that had migrated to the lower surface of the filters was counted under a microscope.

Measurement of Thrombin Activity—Thrombin activity in FCS, CS, and on cells was measured by the method of Kawabata et al. (33). A 10 µl volume of 10% FCS or CS was mixed with 90 µl of reaction buffer containing 50 mM Tris-HCl, pH 8.0, 100 mM NaCl, and 10 mM $CaCl_2$, with or without hirudin (0.5 unit/ml). Packed cells (1×10^6 cells) were suspended in 100 µl of reaction buffer with or without hirudin (0.5 unit/ml). After adding 1 µl of 10 mM substrate, Boc-Asp(Obzl)-pro-Arg-MCA solution to the cell suspension, the mixture was incubated for 20 min at 37°C, and the reaction was stopped by adding 600 µl of 0.6 M acetic acid. The fluorescence of the aminomethyl-coumarine released was measured with a fluorospectro-photometer at an excitation wavelength of 380 nm and an emission of 460 nm. A blank solution was prepared by adding 1 µl of substrate solution to the reaction buffer mixed with 600 µl of 0.6 M acetic acid. Thrombin activity was calculated using 1, 2.5, 5 and 10 ng/ml thrombin solutions as standards and subtracting the fluorescence obtained in the presence of hirudin from that in the absence of hirudin. A linear dose-response curve was obtained between 0.5–5 ng/ml of thrombin, and its activity was inhibited by more than 98% by hirudin (0.5 unit/ml). The fluorescence of each sample was within the linear range.

Proliferation Assay—The cell suspension (1×10^5 cells in 4 ml) was seeded on 60-mm diameter culture dishes and incubated with each factor for 18 h. MEM containing 1% FCS was used as the basal medium. The cells were then detached from the culture dishes with 0.25% trypsin/EDTA, treated with MEM containing 10% CS, collected by centrifugation, and counted with a hemocytometer.

Adhesion Assay—Adhesion assays were performed by a modification of the method of Deryugina et al. (34). A 300 µl aliquot of fibronectin (5 µg/ml), prepared as described above, was added to each well of 24-well plates (IWAKI, Japan). The plates were allowed to stand overnight at 4°C, washed with PBS, blocked with 1% BSA in PBS for 1 h at 37°C, and finally washed in PBS. MMT cells (55×10^4 cells) were exposed to each factor in 2 ml of MEM containing 1% FCS for 30 min at 37°C. After washing with 2 ml of MEM, the cell suspensions (1×10^5 cells in 0.38 ml of MEM) were seeded on each well. After incubation for 30 min at 37°C, non-adherent cells were removed by washing with PBS, and the adherent cells were fixed and stained with 0.2% crystal violet in 10% ethanol for 10 min. After three washes with 2 ml of PBS,
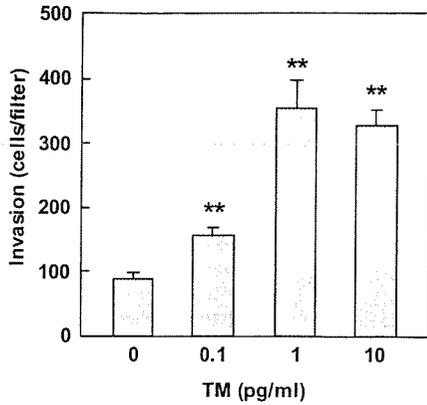
Fig. 1. **Dose dependency of the effect of TM on invasiveness.** MEM containing 1% FCS was used as the basal medium. The concentrations of TM indicated are the concentrations in the lower compartment. The data shown are means ± SD of the data obtained in duplicate wells in three experiments (**$p < 0.01$ vs. control). The deviation in each experiment was less than 10%.
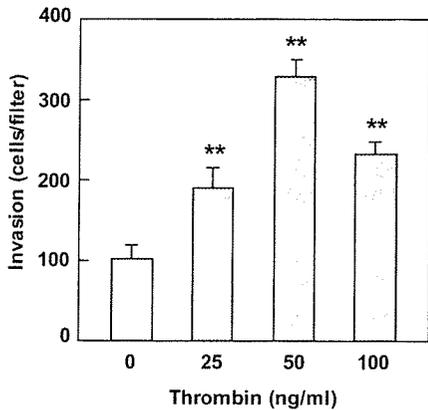

Fig. 2. **Dose dependency of the effect of thrombin on invasiveness.** MEM containing 1% FCS was used as the basal medium. The concentrations of thrombin indicated are the concentrations in the lower compartment. The data shown are means ± SD of data obtained in duplicate wells in three experiments (**$p < 0.01$ vs. control). The deviation in each experiment was less than 10%.

the dye was extracted in an end-over-end mixer with 600 μl of 50% ethanol in 50 mM sodium phosphate (pH 4.5) for 10 min, and absorbance was measured at 540 nm. The correlation between absorbance and cell number was confirmed in a preliminary experiment.

Chemotaxis Assay—Chemotaxis . assays were performed with control inserts (Collaborative Biomedical Products, Bedford, MA, USA) in a similar manner to the invasion assay described above. The control inserts were not coated with Matrigel. MEM containing 1% FCS was used as the basal medium. The control inserts were pre-coated with fibronectin (5 μg/ml) as described for the pre-coating of the Matrigel invasion chamber in the thrombin-activity-depleted assay system.

Iodination of Thrombin and Determination of Binding—Thrombin was iodinated to a specific activity of 19.1 × 10^{7} cpm/μg by the chloramine T method as described previously (*35–36*). After precoating 24-well plates with fibronectin (5 μg/ml) as described above, the cell suspen-
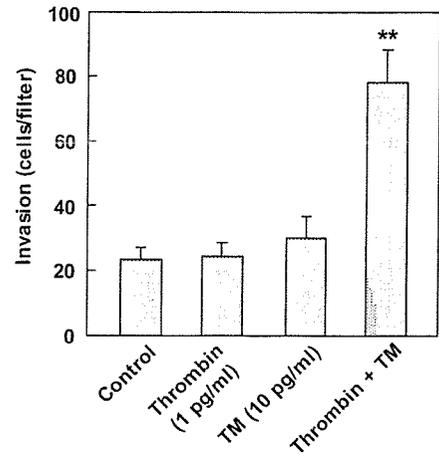

Fig. 3. **Effect of TM and thrombin on invasiveness in the thrombin-activity-depleted assay system.** Cells on which thrombin activity was depleted were used in the experiment. MEM containing 0.1% BSA was used as the basal medium. The data shown are means ± SD of data obtained in duplicate wells in three experiments (**$p < 0.01$ vs. control). The deviation in each experiment was less than 10%.

sions (1.22 × 10^{5} cells in 0.45 ml of MEM) were seeded into each well and incubated in a humidified chamber at 37°C under 5% CO_2 for 2 h. The cells were then washed with 0.4 ml of MEM containing 15 mM Hepes (pH 7.2) and 0.1% BSA and incubated for 1.5 h at 37°C in the same buffer with various concentrations of [^{125}I]-thrombin in the presence or absence of a 100-fold excess amount of unlabeled thrombin. After washing the cells four times with the same ice-cold buffer, the cells were solubilized with 0.4 ml of 1 N NaOH for 1 h at 37°C. Specific binding was calculated as the difference between total binding and nonspecific binding.

RESULTS

Effect of TM on Invasiveness—Figure 1 shows the effects of TM on the invasive activity of MMT cells in the presence of 1% FCS. TM significantly stimulated invasive activity in a dose-dependent manner, resulting in an approximately 3-fold stimulation at 1–10 pg/ml. Figure 2 shows the effects of thrombin used as a positive control. Thrombin also stimulated invasive activity in a dose-dependent manner.

On the basis of these findings, we investigated the possibility that the stimulation of invasion by TM might be dependent on thrombin that may have been introduced into the assay system as described below. First, thrombin activity in the assay system was measured. The thrombin concentrations in freshly prepared 10% FCS and CS measured by the thrombin activity assay were 200 pg/ml and 2.8 ng/ml, respectively. The amount of thrombin on the cells measured in a similar manner was 35 pg/10[6] cells. Based on these values, the thrombin concentrations in the assay system with or without 1% FCS were estimated to be 24.48 and 4.48 pg/ml, respectively. Second, the action of TM was examined in the thrombin-activity-depleted assay system described in "MATERIALS AND METHODS," and depletion of thrombin activity in the
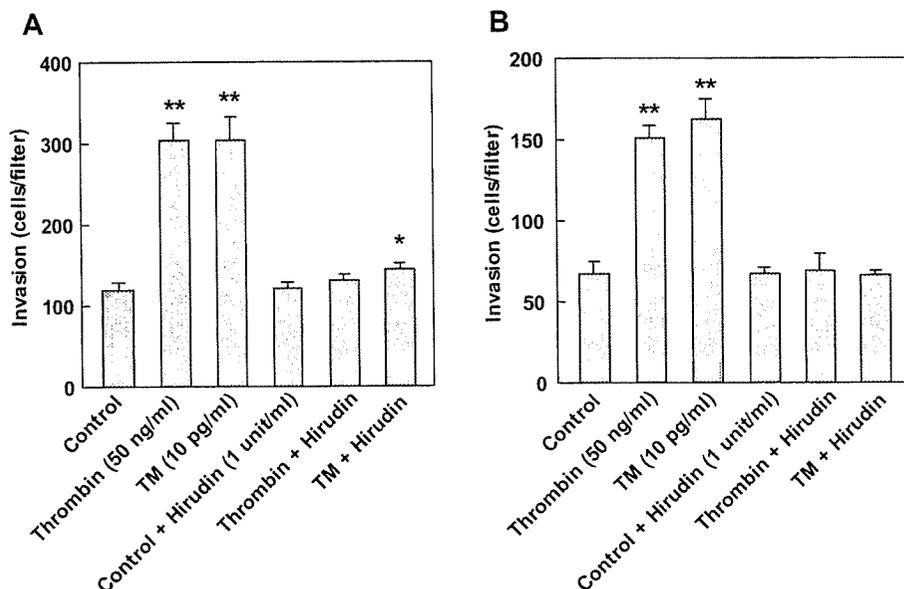
A

B

Fig. 4. **Effect of hirudin on the stimulation of invasion by TM.** (A) MEM containing 1% FCS was used as the basal medium. The indicated concentration of each factor is that in the lower compartment. The data shown are means ± SD of data obtained in duplicate wells in three experiments ($*p < 0.05$ vs. control; $**p < 0.01$ vs. control) (B) MEM containing 0.1% BSA was used as the basal medium. The data shown are means ± SD of data obtained in duplicate wells in three experiments ($**p < 0.01$ vs. control). The deviation in each experiment was less than 10%.

assay system was confirmed by the absence of any detectable thrombin activity on the cells. Figure 3 shows the effects of thrombin (1 pg/ml) and TM (10 pg/ml) on the invasive activity of cells in the thrombin-activity-depleted assay system. While neither thrombin or TM had any effect on invasion, TM plus thrombin stimulated invasion by approximately 3-fold.

Effect of Hirudin on the Stimulation of Invasion by TM—The action of TM was also examined in the presence of the specific thrombin inhibitor hirudin to investigate the possibility described above. Fig. 4, A and B, shows the effects of hirudin on the invasion-stimulating activity of TM in the presence and absence of 1% FCS. We used a 1 unit/ml concentration of hirudin in this experiment, because 50 ng/ml thrombin corresponds to 0.057 unit/ml, and so 1 unit/ml hirudin seemed adequate to inhibit this concentration of thrombin. As expected, hirudin (1 unit/ml) not only inhibited the stimulation by

thrombin to control levels, but the stimulation by TM as well.

Effect of TM on Proliferation—Since tumor cell invasion consists of a series of events, including adhesion to the extracellular matrix (ECM) and chemotaxis, we investigated the effects of TM on these two events to clarify the molecular mechanism of the stimulation of invasive activity by TM. Before investigating the effect of TM on these processes, we investigated its effects on cell proliferation to confirm that the stimulation of invasive activity by TM is not an artifact of the enhancement of cell proliferation.

Figure 5 shows the effects of TM on MMT cell proliferation in the presence of 1% FCS. The numbers of cells in the presence of TM or thrombin did not differ from the numbers in the control cultures.

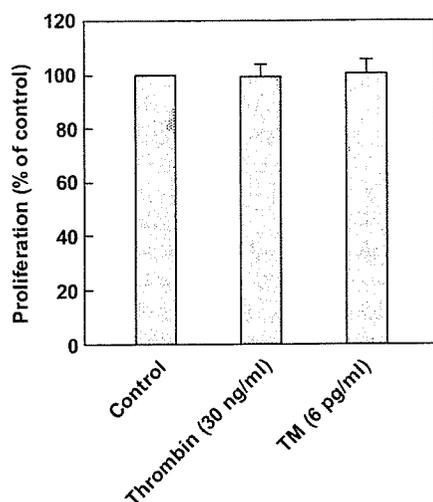*Effect of TM on Adhesion to Fibronectin*—Figure 6 shows the effects of TM on adhesion to fibronectin, a basal lam-

Fig. 5. **Effect of TM on proliferation.** MEM containing 1% FCS was used as the basal medium. The data shown are means ± SD of data obtained in duplicate dishes in three experiments. The deviation in each experiment was less than 10%.
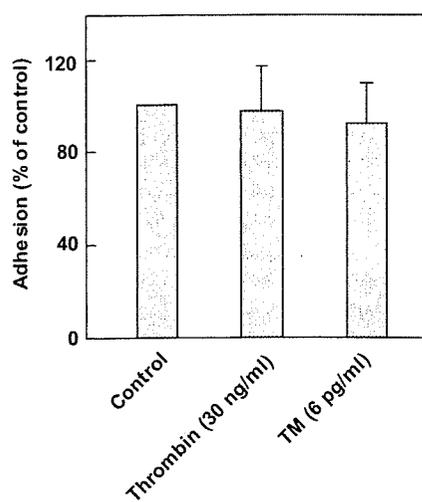

Fig. 6. **Effect of TM on adhesion to fibronectin.** MEM containing 1% FCS was used as the basal medium. The data shown are means ± SD of data obtained in duplicate wells in three experiments. The deviation in each experiment was less than 10%.
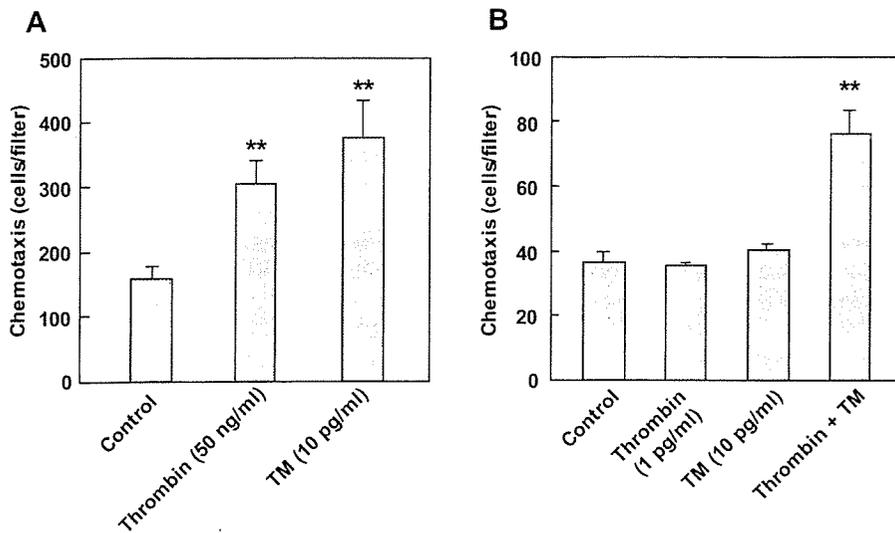
A

B

Fig. 7. **Effect of TM on chemotaxis.** (A) MEM containing 1% FCS was used as the basal medium. The data shown are means ± SD of data obtained in duplicate wells in three experiments (**$p < 0.01$ vs. control). (B) Cells on which thrombin activity was depleted were used in the experiment. MEM containing 0.1% BSA was used as the basal medium. The data shown are means ± SD of data obtained in duplicate wells in three experiments (**$p < 0.01$ vs. control). The deviation in each experiment was less than 10%.

ina component. Neither TM nor thrombin affected adhesion to fibronectin.

Effect of TM on Chemotaxis—Figure 7 (A and B), shows the effects of TM on chemotaxis by MMT cells in the presence of 1% FCS and in the thrombin-activity-depleted assay system, respectively. Both TM (10 pg/ml) and thrombin (50 ng/ml) significantly stimulated chemotaxis by MMT cells by approximately 1.9–2.3-fold in the former system, but neither TM (10 pg/ml) nor thrombin (1 pg/ml) affected chemotaxis in the latter system; TM plus thrombin, on the other hand, stimulated chemotaxis by approximately 2-fold.

Binding of Thrombin—Figure 8 shows the binding curves for specific [125I]-thrombin binding sites on cells in the presence and absence of TM (10 pg/ml). These binding curves show the specific [125I]-thrombin binding to be saturable at approximately 40 ng/ml, and that TM has no effect on the specific binding of [125I]-thrombin. A similar binding experiment was performed in the [125I]-thrombin concentration range of 1–10 pg/ml, but no specific binding was detected independent of the presence or absence of TM, probably because the absolute amount of radioactivity used was too low to be detected as specific binding.

DISCUSSION

In the present study, we show that, at its maximum effective dose, TM stimulates the invasive activity of MMT cells *in vitro* by approximately 3-fold. As far as we know, this is the first time that TM has been shown to stimulate the invasive activity of tumor cells *in vitro*. Similarly, exogenous thrombin causes maximal stimulation of invasion at 50 ng/ml, which is a concentration more than 1,000-fold higher than the maximum effective dose of TM.

Since TM acts as a cofactor for the thrombin-catalyzed activation of protein C and increases the rate of the reaction by >1,000-fold (*8*), the stimulation by TM may have been due to TM interacting with thrombin, which had been introduced into the assay system, and acting as a cofactor for thrombin-stimulated invasion of MMT cells, thus lowering the effective concentration of thrombin. This possibility seems to be supported by the detection of thrombin activity in the assay systems, the requirement

for thrombin for stimulation by TM in the thrombin-activity-depleted assay system, and the inhibition of stimulation by hirudin. It is noteworthy that the thrombin concentration required for stimulation by TM in the thrombin-activity-depleted assay system is more than 20,000-fold less than the concentration required for thrombin to stimulate invasion. On the other hand, the control level was not inhibited by hirudin in the presence of 1% FCS, probably due to the lower thrombin concentration in the assay system compared with the effective concentration of exogenous thrombin.

There have been two studies examining the effect of TM on the invasive activity of tumor cells. Matsushita *et al.* showed that a subcloned human esophageal squamous cell carcinoma line with low TM expression is more invasive than a high TM-expressing clone (*37*). In their study, the action of TM does not seem to be due to an acceleration of its thrombin cofactor activity, because the difference between the cell lines with low and high TM expression with respect to their cofactor activity for protein C activation by thrombin was less than 13% and significantly lower than their TM levels and invasive activities. Hosaka *et al.* showed that TM (10–100 ng/ml)
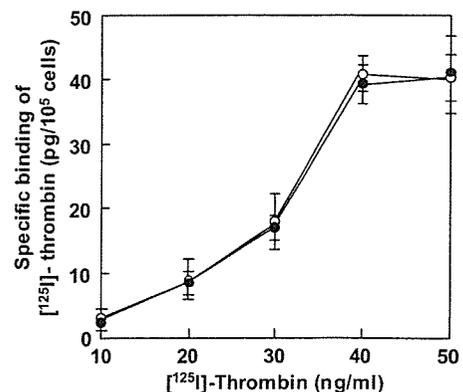

Fig. 8. **Binding of [125I]-thrombin.** Specific binding of [125I]-thrombin to cells in the absence (solid circles) and presence of TM (10 pg/ml) (open circles) was measured. The data shown are representative specific binding curves for [125I]-thrombin binding sites and are means ± SD of data obtained in triplicate wells.

inhibits the invasive activity of mouse melanoma cells *in vitro* (*38*), and TM has also been found to decrease the proliferation of tumor cell lines subcloned from patients with malignant melanomas (*39*). None of these inhibitory effects were inhibited by hirudin.

In contrast to these studies, the present study shows that TM enhances the invasive activity of MMT cells and indicates that the action of TM is entirely dependent on thrombin as described above. Therefore, the mode and mechanism of action of TM in MMT cells seems to be different from its mode and mechanism of action in the squamous cell carcinoma line and melanoma cells.

It is useful to speculate on the role of TM in tumorigenesis based on the findings of our study, because tumor cell invasion through the basement membrane is a critical step in the process of metastasis (*29–30*). Several studies have shown that TM levels in serum increase in patients with certain tumors (*26–28*), as described in the Introduction. Thus, the results of this study suggest that the soluble form of TM may play a positive role in the malignancy of some kinds of tumors, probably by enhancing the metastatic potential of thrombin. On the other hand, TM on the cell surface may act as a negative regulator to thrombin, because thrombin is degraded as the thrombin-TM complex by its internalization after binding to TM on the cell surface (*40*). This possibility may be supported by the findings that the expression level of TM is negatively correlated with the malignancy of some carcinomas (*23–25*), as described in the Introduction.

Tumor cell invasion is a complex process that involves adhesion to ECM, degradation of ECM, and chemotaxis (*41*). Chemotaxis is the essential step in invasion as reviewed by Wells (*42*). The results of the present study show that both TM and thrombin stimulate chemotaxis in the presence of 1% FCS, and that TM plus thrombin stimulate chemotaxis in the thrombin-activity-depleted assay system. Both of these findings are consistent with previous reports that thrombin stimulates chemotaxis (*17, 18*), and the presence of specific binding sites for thrombin on cells indicates that these actions are mediated by thrombin receptors.

However, other actions of thrombin may also be involved in the stimulation of tumor cell invasion, because the enhancement of chemotaxis alone is insufficient to account for the increase in tumor cell invasion. One such other possible action of thrombin is the stimulation of the matrix metalloprotease (MMP)–mediated degradation of a variety of ECM proteins, including collagens type IV, V, VII, and X, fibronectin, laminin (*43–47*), elastin (*48–49*), proteoglycans (*49–51*), and entactin (*52*). Several reports have indicated that thrombin increases the active forms of MMP-2 and MMP-9 (*53–59*), and plays important roles in the enhancement of tumor cell invasion and metastasis (*34, 60–68*). There are also reports that thrombin stimulates the release of MMP-2 (*69*), the expression of MMP-1 and MMP-3 (*70*), and the expression of MMP-9 mRNA (*71*). Another possible action is the stimulation of MMP-independent degradation of ECM. This possibility appears to be supported by the finding that thrombin stimulates the expression of urokinase-type plasminogen activator, a factor involved in the degradation of ECM protein (*72*), and stimulates the heparinase-mediated release of heparan sulfate from ECM (*73*).

In conclusion, the results of this study show that TM stimulates the invasive activity of MMT cells, probably by acting as a cofactor for the thrombin-stimulated invasion of cells mediated by thrombin receptors, and by lowering the effective concentration of thrombin. Further, the results indicate that the stimulation is mainly caused by an enhancement of chemotaxis.

REFERENCES

1. Esmon, C.T. and Owen, W.G. (1981) Identification of an endothelial cell cofactor for thrombin-catalyzed activation of protein C. *Proc. Natl Acad. Sci. USA* **78**, 2249–2252
2. Esmon, C.T. (1989) The roles of protein C and thrombomodulin in the regulation of blood coagulation. *J. Biol. Chem.* **264**, 4743–4746
3. Ishii, H. and Majerus, P.W. (1985) Thrombomodulin is present in human plasma and urine. *J. Clin. Invest.* **76**, 2178–2181
4. Molinari, A., Giorgetti, C., Lansen, J., Vaghi, F., Orsini, G., Faioni, E.M., and Mannucci, P.M. (1992) Thrombomodulin is a cofactor for thrombin degradation of recombinant single-chain urokinase plasminogen activator "in vitro" and in a perfused rabbit heart model. *Thromb. Haemost.* **67**, 226–232
5. Bajzar, L., Morser, J., and Nesheim, M. (1996) TAFI, or plasma procarboxypeptidase B, couples the coagulation and fibrinolytic cascades through the thrombin-thrombomodulin complex. *J. Biol. Chem.* **271**, 16603–16608
6. Pekovich, S.R., Bock, P.E., and Hoover, R.L. (2001) Thrombin-thrombomodulin activation of protein C facilitates the activation of progelatinase A. *FEBS Lett.* **494**, 129–132
7. Esmon, N.L., Carroll, R.C., and Esmon, C.T. (1986) Thrombomodulin blocks the ability of thrombin to activate platelets. *J. Biol. Chem.* **258**, 12238–12242
8. Esmon, C.T., Esmon, N.L., and Harris, K.W. (1983) Complex formation between thrombin and thrombomodulin inhibits both thrombin-catalyzed fibrin formation and factor V activation. *J. Biol. Chem.* **257**, 7944–7947
9. Parkinson, J.F., Bang, N.U., and Garcia, J.G. (1993) Recombinant human thrombomodulin attenuates human endothelial cell activation by human thrombin. *Arterioscler. Thromb.* **13**, 1119–1123
10. Li, J., Garnette, C.S., Cahn, M., Claytor, R.B., Rohrer, M.J., Dobson, J.G. Jr., Gerlitz. B., and Cutler, B.S. (2000) Recombinant thrombomodulin inhibits arterial smooth muscle cell proliferation induced by thrombin. *J. Vasc. Surg.* **32**, 804–813
11. Lafay, M., Laguna, R., Le Bonniec, B.F., Lasne, D., Aiach, M., and Rendu, F. (1998) Thrombomodulin modulates the mitogenic response to thrombin of human umbilical vein endothelial cells. *Thromb. Haemost.* **79**, 848–852
12. Nierodzik, M.L., Plotkin, A., Kajumo, F., and Karpatkin, S. (1991) Thrombin stimulates tumor-platelet adhesion *in vitro* and metastasis *in vivo*. *J. Clin. Invest.* **87**, 229–236
13. Nierodzik, M.L., Kajumo, F., and Karpatkin, S. (1992) Effect of thrombin treatment of tumor cells on adhesion of tumor cells to platelets *in vitro* and tumor metastasis *in vivo*. *Cancer Res.* **52**, 3267–3272
14. Esumi, N., Fan, D., and Fidler, J.I. (1991) Inhibition of murine melanoma experimental metastasis by recombinant desulfatohirudin, a highly specific thrombin inhibitor. *Cancer Res.* **51**, 4549–4556
15. Wojtukiewicz, M.Z., Tang, D.G., Ben-Josef, E., Renaud, C., Walz, D.A., and Honn, K.V. (1995) Solid tumor cells express functional 'tethered ligand' thrombin receptor. *Cancer Res.* **55**, 698–704
16. Even-Ram, S., Uziely. B., Cohen, P., Grisaru-Granovsky, S., Maoz, M., Ginzburg, Y., Reich, R., Vlodavsky, I., and Bar-

Shavit, R. (1998) Thrombin receptor overexpression in malignant and physiological invasion processes. *Nat. Med.* **4**, 909–914

17. Hernandez-Rodriguez, N.A., Correa, E., Contreras-Paredes, A., and Green, L. (1999) Evidence that thrombin present in lungs of patients with pulmonary metastasis may contribute to the development of the disease. *Lung Cancer* **26**, 157–167

18. Henrikson, K.P., Salazar, S.L., Fenton, J.W. II., and Pentecost, B.T. (1999) Role of thrombin receptor in breast cancer invasiveness. *Br. J. Cancer* **79**, 401–406

19. Ogawa, H., Yonezawa, S., Maruyama, I., Matsushita, Y., Tezuka, Y., Toyoyama, H., Yanagi, M., Matsumoto, H., Nishijima, H., Shimotakahara, T., Aikou, T., and Sato, E. (2000) Expression of thrombomodulin in squamous cell carcinoma of the lungs: its relationship to lymph node metastasis and prognosis of the patients. *Cancer Lett.* **149**, 95–103

20. Takebayashi, Y., Yamada, K., Maruyama, I., Fujii, R., Akiyama, S., and Aikou, T. (1995) The expression of thymidine phosphorylase and thrombomodulin in human colorectal carcinomas. *Cancer Lett.* **92**, 1–7

21. Ordonez, N.G. (1997) Value of thrombomodulin immunostaining in the diagnosis of transitional cell carcinoma: a comparative study with carcinoembryonic antigen. *Histopathology* **31**, 517–524

22. Ordonez, N.G. (1998) Thrombomodulin expression in transitional cell carcinoma. *Am. J. Clin. Pathol.* **110**, 385–390

23. Matsumoto, M., Natsugoe, S., Nakashima, S., Shimada, M., Nakano, S., Kusano, C., Baba, M., Takao, S., Matsushita, Y., and Aikou, T. (2000) Biological evaluation of undifferentiated carcinoma of the esophagus. *Ann. Surg. Oncol.* **7**, 204–209

24. Suehiro, T., Shimada, M., Matsumata, T., Taketomi, A., Yamamoto, K., and Sugimachi, K. (1995) Thrombomodulin inhibits intrahepatic spread in human hepatocellular carcinoma. *Hepatology* **21**, 1285–1290

25. Wilhelm, S., Schmitt, M., Parkinson, J., Kuhn, W., Graeff, H., and Wilhelm O.G. (1998) Thrombomodulin, a receptor for the serine protease thrombin, is decreased in primary tumors and metastases but increased in ascitic fluids of patients with advanced ovarian cancer FIGO IIIc. *Int. J. Oncol.* **13**, 645–651

26. Lindahl, A.K., Boffa, M.C., and Abildgaard, U. (1993) Increased plasma thrombomodulin in cancer patients. *Thromb. Haemost.* **69**, 112–114

27. Boffa, M.C., Lapeyrere, C., Berard, M., Lindahl, A.K., Flageul, B., Chemaly, P., Abildgaard, U., and Dubertret, L. (1994) Plasma thrombomodulin level in malignancy varies according to the tumor type. *Nouv. Rev. Fr. Hematol.* **36**, S87–88

28. Salmaggi, A., Eoli, M., Frigerio, S., Ciusani, E., Silvani, A., and Boiardi, A. (1999) Circulating intercellular adhesion molecule-1 (ICAM-1), vascular cell adhesion molecule-1 (VCAM-1) and plasma thrombomodulin levels in glioblastoma patients. *Cancer Lett.* **146**, 169–172

29. Liotta, L.A. (1986) Tumor invasion and metastases-role of the extracellular matrix: Rhoads Memorial Award lecture. *Cancer Res.* **46**, 1–7

30. Terranova, V.P., Hujanen, E.S., and Martin, G.R. (1986) Basement membrane and the invasive activity of metastatic tumor cells. *J. Natl Cancer Inst.* **77**, 311–316

31. Gomi, K., Zushi, M., Honda, G., Kawahara, S., Matsuzaki, O., Jr., Kanabayashi, T., Yamamoto, S., Maruyama, I., and Suzuki, K. (1990) Antithrombotic effect of recombinant human thrombomodulin on thrombin-induced thromboembolism in mice. *Blood* **75**, 1396–1399

32. Niimi, S., Oshizawa, T., Naotsuka, M., Ohba, S., Yokozawa, A., Murata, T., and Hayakawa, T. (2002) Establishment of a standard assay method for human thrombomodulin and determination of the activity of the Japanese reference standard. *Biologicals* **30**, 69–76

33. Kawabata, S., Miura, T., Morita, T., Kato, H., Fujikawa, K., Iwanaga, S., Takada, K., Kimura, T., and Sakakibara, S. (1988) Highly sensitive peptide-4-methylcoumaryl-7-amide substrates for blood-clotting proteases and trypsin. *Eur. J. Biochem.* **172**, 17–25

34. Deryugina, E.I., Luo, G.X., Reisfeld, R.A., Bourdon, M.A., and Strongin, A. (1997) Tumor cell invasion through matrigel is regulated by activated matrix metalloproteinase-2. *Anticancer Res.* **17**, 3201–3210

35. Greenwood, F.C., Hunter, W.M., Glover, J.S. (1963) The preparation of ^{131}I-labelled human growth hormone of high specific radioactivity. *Biochem. J.* **89**, 114–123

36. Haeuptle, M.T., Aubert, M.L., Djiane J., Kraehenbuhl, J.P. (1983) Binding sites for lactogenic and somatogenic hormones from rabbit mammary gland and liver. *J. Biol. Chem.* **258**, 305–314

37. Matsushita, Y., Yoshiie, K., Imamura, Y., Ogawa, H., Imamura, H., Takao, S., Yonezawa, S., Aikou, T., Maruyama, I., and Sato, E. (1998) A subcloned human esophageal squamous cell carcinoma cell line with low thrombomodulin expression showed increased invasiveness compared with a high thrombomodulin-expressing clone—thrombomodulin as a possible candidate for an adhesion molecule of squamous cell carcinoma. *Cancer Lett.* **127**, 195–201

38. Hosaka, Y., Higuchi, T., Tsumagari, M., and Ishii, H. (2000) Inhibition of invasion and experimental metastasis of murine melanoma cells by human soluble thrombomodulin. *Cancer Lett.* **161**, 231–240

39. Zhang, Y., Weiler-Guettler, H., Chen, J., Wilhelm, O., Deng, Y., Qiu, F., Nakagawa, K., Klevesath, M., Wilhelm, S., Bohrer, H., Nakagawa, M., Graeff, H., Martin, E., Stern, D.M., Rosenberg, R.D., Ziegler, R., and Nawroth, P.P. (1998) Thrombomodulin modulates growth of tumor cells independent of its anticoagulant activity. *J. Clin. Invest.* **101**, 1301–1309

40. Maruyama, I. and Majerus, P.W. (1985) The turnover of thrombin-thrombomodulin complex in cultured human umbilical vein endothelial cells and A549 lung cancer cells. Endocytosis and degradation of thrombin. *J. Biol. Chem.* **260**, 15432–15438

41. Hart, I.R., Goode, N.T., and Wilson, R.E. (1989) Molecular aspects of the metastatic cascade. *Biochim. Biophys. Acta* **989**, 65–84

42. Wells, A. (2000) Tumor invasion: role of growth factor-induced cell motility. *Adv. Cancer Res.* **78**, 31–101

43. Matrisian, L.M. (1990) Metalloproteinases and their inhibitors in matrix remodeling. *Ternds Genet.* **6**, 121–125

44. Collier, I.E., Wilhelm, S.M., Eisen, A.Z., Marmer, B.L., Grant. G.A., Seltzer. J.L., Kronberger, A., He. C.S., Bauer, E.A., and Goldberg, G.I. (1988) H-ras oncogene-transformed human bronchial epithelial cells (TBE-1) secrete a single metalloprotease capable of degrading basement membrane collagen. *J. Biol. Chem.* **263**, 6579–6587

45. Wilhelm, S.M., Collier, I.E., Marmer, B.L., Eisen, A.Z., Grant, G.A., and Goldberg, G.I. (1989) SV40-transformed human lung fibroblasts secrete a 92-kDa type IV collagenase which is identical to that secreted by normal human macrophages. *J. Biol. Chem.* **264**, 17213–17221

46. Fessler, L.I., Duncan, K.G., Fessler, J.H., Salo, T., and Tryggvason, K. (1984) Identification of the procollagen IV cleavage products produced by a specific tumor collagenase. *J. Biol. Chem.* **259**, 9783–9789

47. Woessner, J.F. Jr. (1991) Matrix metalloproteinases and their inhibitors in connective tissue remodeling. *FASEB J.* **5**, 2145–2154

48. Senior, R.M., Griffin, G.L., Fliszar, C.J., Shapiro, S.D., Goldberg, G.I., and Welgus, H.G. (1991) Human 92- and 72-kilodalton type IV collagenases are elastases. *J. Biol. Chem.* **266**, 7870–7875

49. Murphy, G., Cockett, M.I., Ward, R.V., and Docherty, A.J. (1991) Matrix metalloproteinase degradation of elastin, type IV collagen and proteoglycan. A quantitive comparison of the activities of 95 kDa and 72 kDa gelatinases, stromelysins-1 and -2 and punctuated metalloproteinae (PUMP). *Biochem. J.* **277**, 277–279

50. Nguyen, Q., Murphy, G., Hughes, C.E., Mort, J.S., and Roughley, P.J. (1993) Matrix metalloproteinases cleave at two distinct sites on human cartilage link protein. *Biochem. J.* **295**, 595–598

51. Fosang, A.J., Last, K., Knauper, V., Neame, P.J., Murphy, G., Hardingham, T.E., Tschesche, H., and Hamilton, J.A. (1993) Fibroblast and neutrophil collagenases cleave at two sites in the cartilage aggrecan interglobular domain. *Biochem. J.* **295**, 273–276

52. Sires, U.I., Griffin, G.L., Broekelmann, T.J., Mecham, R.P., Murphy, G., Chung, A.E., Welgus, H.G., and Senior, R.M. (1993) Degradation of entactin by matrix metalloproteinases. Susceptibility to matrilysin and identification of cleavage sites. *J. Biol. Chem.* **268**, 2069–2074

53. Zucker, S., Conner, C., DiMassmo, B.I., Ende, H., Drews, M., Seiki, M., and Bahou, W.F. (1995) Thrombin induces the activation of progelatinase A in vascular endothelial cells. Physiologic regulation of angiogenesis. *J. Biol. Chem.* **270**, 23730–23738

54. Galis, Z.S., Kranzhofer, R., Fenton, J.W. II., and Libby, P. (1997) Thrombin promotes activation of matrix metalloproteinase-2 produced by cultured vascular smooth muscle cells. *Arterioscler. Thromb. Vasc. Biol.* **17**, 483–489

55. Nguyen, M., Arkell, J., and Jackson, C.J. (1999) Thrombin rapidly and efficiently activates gelatinase A in human microvascular endothelial cells via a mechanism independent of active MT1 matrix metalloproteinase. *Lab. Invest.* **79**, 467–475

56. Pekovich, S.R., Bock, P.E., and Hoover, R.L. (2001) Thrombin-thrombomodulin activation of protein C facilitates the activation of progelatinase A. *FEBS Lett.* **694**, 129–132

57. Lafleur, M.A., Hollenberg, M.D., Atkinson. S.J., Knauper, V., Murphy, G., and Edwards, D.R. (2001) Activation of pro-(matrix metalloproteinase-2) (pro-MMP-2) by thrombin is membrane-type-MMP-dependent in human umbilical vein endothelial cells and generates a distinct 63 kDa active species. *Biochem. J.* **357**, 107–115

58. Maragoudakis, M.E., Kraniti, N., Giannopoulou, E., Alexopoulos, K., and Matsuokas, J. (2001) Modulation of angiogenesis and progelatinase A by thrombin receptor mimetics and antagonists. *Endothelium* **8**, 195–205

59. Liu, Y., Gilcrease, M.Z., Henderson, Y., Yuan, X.H., Clayman, G.L., and Chen, Z. (2001) Expression of protease-activated receptor 1 in oral squamous cell carcinoma. *Cancer Lett.* **169**, 173–180

60. Stetler-Stevenson, W.G., Aznavoorian, S., and Liotta, L.A. (1993) Tumor cell interactions with the extracellular matrix during invasion and metastasis. *Annu. Rev. Cell. Biol.* **9**, 541–573

61. Himelstein, B.P., Canete-Soler, R., Bernhard, E.J., Dilks, D.W., and Muschel, R.J. (1994) Metalloproteinases in tumor progression: the contribution of MMP-9. *Invasion Metastasis.* **14**, 246–258

62. Bernhard, E.J., Gruber, S.B., and Muschel, R.J. (1994) Direct evidence linking expression of matrix metalloproteinase 9 (92-kDa gelatinase/collagenase) to the metastatic phenotype in transformed rat embryo cells. *Proc. Natl Acad. Sci. USA* **91**, 4293–4297

63. MacDougall, J.R., and Matrisian. L.M. (1995) Contribution of tumor and stromal matrix metalloroteinases to tumor progression, invasion and metastasis. *Cancer Metastasis Rev.* **14**, 351–362

64. Hua, J. and Muschel, R.J. (1996) Inhibition of matrix metalloproteinase 9 expression by a ribozyme blocks metastasis in a rat sarcoma model system. *Cancer Res.* **56**, 5279–5284

65. Kim, J., Yu, W., Kovalski, K., and Ossowski, L. (1998) Requirement for specific proteases in cancer cell intravasation as revealed by a novel semiquantitative PCR-based assay. *Cell* **94**, 353–362

66. Hahn-Dantona, E., Ramos-DeSimone, N., Sipley, J., Nagase, H., French, D.L., and Quigley, J.P. (1999) Activation of proMMP-9 by a plasmin/MMP-3 cascade in a tumor cell model. Regulation by tissue inhibitors of metalloproteinases. *Ann. N. Y. Acad. Sci.* **878**, 372–387

67. John, A. and Tuszynski, G. (2001) The role of matrix metalloproteinases in tumor angiogenesis and tumor metastasis. *Pathol. Oncol. Res.* **7**, 14–23

68. Giannelli, G. and Antonaci, S. (2002) Gelatinases and their inhibitors in tumor metastasis: from biological research to medical applications. *Histol. Histopathol.* **17**, 339–345

69. Fernandez-Patron, C., Zhang, Y., Radomski, M.W., Hollenberg, M.D., and Davidge, S.T. (1999) Rapid release of matrix metalloproteinase (MMP)-2 by thrombin in the rat aorta: modulation by protein tyrosine kinase/phosphatase. *Thromb. Haemost.* **82**, 1353–1357

70. Duhamel-Clérin, E., Orvain, C., Lanza, F., Cazenave, J.P., and Klein-Soyer, C. (1997) Thrombin receptor-mediated increase of two matrix metalloproteinases, MMP-1 and MMP-3, in human endothelial cells. *Arterioscler. Thromb. Vasc. Biol.* **17**, 1931–1938

71. Liu, W.H., Chen, X.M., and Fu, B. (2000) Thrombin stimulates MMP-9 mRNA expression through AP-1 pathway in human mesangial cells. *Acta. Pharmacol. Sin.* **21**, 641–645

72. Yoshida, E., Verrusio, E.N., Mihara, H., Oh, D., and Kwaan, H.C. (1994) Enhancement of the expression of urokinase-type plasminogen activator from PC-3 human prostate cancer cells by thrombin. *Cancer Res.* **54**, 3300–3304

73. Benezra, M., Vlodavsky, I., and Bar-Shavit, R. (1992) Thrombin enhances degradation of heparan sulfate in the extracellular matrix by tumor cell heparanase. *Exp. Cell Res.* **201**, 208–215

Expression of Annexin A3 in Primary Cultured Parenchymal Rat Hepatocytes and Inhibition of DNA Synthesis by Suppression of Annexin A3 Expression Using RNA Interference

Shingo Niimi,*,[a] Mizuho Harashima,[b] Masaru Gamou,[b] Masashi Hyuga,[a] Taiichiro Seki,[b] Toyohiko Ariga,[b] Toru Kawanishi,[a] and Takao Hayakawa[c]

[a] *Division of Biological Chemistry and Biologicals, National Institute of Health Sciences; 1–18–1 Kamiyoga, Setagaya-ku, Tokyo 158–8501, Japan:* [b] *Department of Nutrition and Physiology, Nihon University College of Bioresource Sciences; Kameino, Fujisawa 252–8510, Japan: and* [c] *Deputy Director General, National Institute of Health Sciences; 1–18–1 Kamiyoga, Setagaya-ku, Tokyo 158–8501, Japan.*

Annexin A3 is a member of the lipocortin/annexin family, which binds to phospholipids and membranes in a Ca^{2+}-dependent manner. Although annexin A3 has various functions *in vitro*, its cellular significance is completely unknown. Annexin A3 is not found in rat liver *in vivo*. In the present study, we investigated the expression of annexin A3 in primary cultured parenchymal rat hepatocytes. Annexin A3 protein was detected in 48-h, but not 2.5-h, cultured hepatocytes using Western blot analysis. The annexin A3 level further increased after an additional 24 h of culture. Annexin A3 mRNA was not detected in 2.5-h cultured hepatocytes but was detected 22 h after the start of culture by RT-PCR analysis, reaching a maximum value after 48 h of culture. To define the role of Annexin A3 in DNA synthesis, RNA interference was used to reduce annexin III gene expression in hepatocytes. The transfection of small interfering RNAs targeting annexin A3 in the hepatocytes reduced the corresponding mRNA and protein expression by approximately 80% and more than 90%, respectively, at 24 h after transfection. In the annexin A3 small interfering RNAs-transfected cells, DNA synthesis, as assessed by [^{3}H]thymidine incorporation, decreased by approximately 70% not only in the control cultures, but also in the hepatocyte growth factor- or epidermal growth factor-treated cells. These findings show that annexin A3 is expressed in primary cultured parenchymal rat hepatocytes and that the suppression of annexin A3 expression using RNA interference inhibits DNA synthesis.

Key words   annexin A3; RNAi; DNA synthesis; primary cultured hepatocyte; hepatocyte growth factor (HGF); epidermal growth factor (EGF)

Annexin (Anx) A3 is also called "lipocortin 3" or "placental anticoagulant protein 3" (PAP-III)[1] and is a member of the lipocortin/annexin family, which binds to phospholipids and membranes in a Ca^{2+}-dependent manner.[2—4] AnxA3 has been shown to have anticoagulant and anti-phospholipase A_2 properties *in vitro*[5] and to promote the Ca^{2+}-dependent aggregation of isolated specific granules from human neutrophils.[6] Although the physiological functions of other annexins have been recently clarified in knock-out and transgenic models,[7—14] the functions of AnxA3 are completely unknown.[15]

Recently, we found that AnxA3 protein and its mRNA are not expressed in isolated parenchymal rat hepatocytes.[16,17] Consistent with these findings, AnxA3 protein and its mRNA are not detectable by Western blot analysis and Northern blot analysis in rat liver.[18—21] However, there have been no reports on the behavior of AnxA3 in primary cultured parenchymal rat hepatocytes. In the present study, we investigated the expression and function of AnxA3 in cultured parenchymal rat hepatocytes.

MATERIALS AND METHODS

Materials   Recombinant human hepatocyte growth factor (HGF) was purchased from R&D systems (Minneapolis, MN, U.S.A.). Mouse epidermal growth factor (EGF) was purchased from Wako (Osaka, Japan). [^{3}H]thymidine (79.9 Ci/mmol) was purchased from PerkinElmer (Boston, MA, U.S.A.). Rabbit anti-human ANXA3 antibody serum

was a generous gift from Dr. F. Russo-Marie and Dr. C. Raguenness-Nicol.

Cell Isolation and Monolayer Cultures   Parenchymal hepatocytes were isolated from adult male Wistar rats, weighing 180—200 g, by *in situ* perfusion of the liver with collagenase.[22] All animal care and procedure protocols were approved by the institutional care committee. The cells were then suspended at a density of 2.5×10^5 cells/ml in Williams E medium (WE) containing 5% fetal bovine serum and 1 nM insulin and cultured at a density of 0.5×10^5 cells/cm^2 in a 6 cm dish and a 48-well microplate precoated with collagen type-1 AC in a humidified chamber at 37 °C in 5% CO_2 and 30% O_2 in air. Cells plated in the 6-cm dish and 48-well microplate were used to prepare total cellular extracts or total RNA and to measure DNA synthesis, respectively. After 2.5 h of culture, the medium was replaced with a serum- and hormone-free medium containing aprotinin (1 µg/ml).

Western Blot Analysis   Cell lysates were prepared using a modification of a previously described method.[23] The cells were washed with phosphate-buffered saline (PBS) followed by buffer A (50 mM Tris–HCl [pH 7.5], 150 mM NaCl, and 10 mM EDTA). The cells were then harvested after the addition of 20 µl of buffer A. The cells were suspended, shaken for 15 min at room temperature, and sonicated five times for 15 s each time while in an ice bath after the addition of 1/5 [v/v] of 5×buffer A containing 2.5% Triton X-100 and 1/100 [v/v] of a protease inhibitor cocktail (SIGMA). After centrifugation at $100000 \times g$, the cytosolic fraction (about 25 µg) was subjected to sodium dodecyl sulfate-polyacrylamide gel

electrophoresis on a 10% gel and electroblotted to a PVDF membrane (GVHP; Millipore). After blocking the membrane with 5% skimmed milk, a Western blot analysis was performed using rabbit anti-human AnxA3 antibody serum at a dilution of 1 : 18000; detection was performed using the ECL detection system (Amersham Bioscience).

Reverse Transcription Polymerase Chain Reaction Analysis Total RNA was exctracted from the cells using Trizol reagent (Invitrogen) according to the manufacturer's protocols. Approximately 3 μg of RNA per sample was reverse-transcribed using the THERMOSCRIPT^{TM} RT-PCR System (Invitrogen) and oligo(dT)$_{20}$ in a final volume of 40 μl, according to the manufacturer's protocols. Subsequently, 1 μl of cDNA was polymerase chain reaction (PCR)-amplified using the THERMOSCRIPT^{TM} RT-PCR System (Invitrogen) in a final volume of 20 μl per reaction, according to the manufacturer's protocols, for 14—23 cycles of denaturation for 30 s at 94 °C, annealing for 30 s at 60 °C, and polymerization for 1 min at 72 °C using Anx AlII or glyceraldehyde 3-phosphate dehydrogenase (GAPDH) cDNA specific primers under linear conditions. The PCR products were separated on a 2% agarose gel, stained with SYBR Green I, and visualized and analyzed with a FluoroImager 595 (Amersham Bioscience). A computer assisted-analyzer was used to quantitatively analyze the signals, and the signals were normalized to the signal of a house keeping gene, the gene coding GAPDH. The sequences of the AnxA3 primers were as follows: 5'-CAAATTCACCGAGATCCTGT-3' and 5'-TGCTGGAGTGCTGTACGAAA-3'. The sequences of the GAPDH primers were as follows: 5'-ACCACAGTCCAT-GCCATCAC-3' and 5'-TCCACCACCTGTTGCTGTA-3'.[24] The PCR product specificity was confirmed by DNA sequence analysis using an ABI Prism 377 DNA Sequencer (Applied Biosystems, Foster City, CA, U.S.A.).

Preparation and Transfection of Small Interfering RNAs Targeting AnxA3 Small interfering RNAs (siRNAs) targeting rat AnxA3 were designed according to the guidelines of the "Dharmacon siDESIGN Center" (www.dharmacon.com) and obtained from Dharmacon Research (Lafayette) in annealed and lyophilized forms. The target sequences were localized at positions, 493 and 690 bps downstream of the start codon. The sequences of each siRNA pair were as follows: AnxA3 siRNA 1, 5'-GAG ACG AAA GCC UGA AAG UdTdT-3' and ACU UUC AGG CUU UCG UCU cdTdT-3'; ANXA3 siRNA 2, 5'-GGA GAA UUA UCU GGG CAU UdTdT-3' and AAU GCC CAG AUA AUUCUC cdTdT-3; and control siRNA, 5'-ACU CUA UCU GCA CGC UGA CUU-3' and 5'-P G UCA GCG UGC AGA UAG AGU UU-3'. No homology between any relevant mammalian gene and the control siRNA was observed. These siRNAs were dissolved in an RNase-free solution provided by Dharmacon Research at a concentration of 20 μM. After 20 h of cell culture, the medium was replaced with WE containing aprotinin (1 μg/ml) immediately prior to transfection. Transfection with siRNA was performed using SiFector (B-bridge), according to the user guidelines. Sixty microliters of both AnxA3 siRNA 1 and 2 were diluted with OPTI-MEM (Invitrogen) to a final volume of 400 μl. Sixty-four microliters of SiFector was also diluted in OPTI-MEM to a final volume of 400 μl, then suspended and incubated at room temperature for 5 min. Next, the diluted siRNA was combined with SiFector, and the mixture was incubated at room temperature to allow the siRNA-SiFector complex to form. Eight hundred microliters of the siRNA-SiFector complex was added to the cultures (6-cm dish). For the 48-well plates, the siRNA-SiFector complex was prepared as described above except that the volume of each solution per well was scaled down to 1/16.

Measurement of [^{3}H]thymidine Incorporation After 20 h of culture, the medium was replaced with hormone-free medium containing aprotinin (1 μg/ml) and 0.1% bovine serum albumin (BSA), and EGF (2 ng/ml) or HGF (20 ng/ml) was added. After 1 h, 50 μl of siRNA-SiFector complex, prepared as described above, was added to the wells. After another 24 h, [^{3}H]thymidine (0.626 μCi) and thymidine (676.6 ng) were added, and 10 μg/ml of aphidicolin was added to some wells at the same time. The cells were then cultured for another 24 h. [^{3}H]thymidine incorporation was measured as described previously.[25] The difference between the radioactivity in the hot-trichloroacetic acid soluble fraction with and without aphidicolin was calculated as dpm/mg protein. Cell protein was measured using a previously described method,[26] with BSA used as a standard.

RESULTS

Expression of AnxA3 during Culture At first, we investigated the expression of AnxA3 in primary cultured parenchymal rat hepatocytes. AnxA3 protein was not detected by Western blot analysis 2.5 and 24 h after the start of culture but was detected after 48 h of culture (Fig. 1A). The level after 72 h of culture was approximately 1.6-fold higher than that after 48 h of culture (Fig. 1B). AnxA3 mRNA was not detected by reverse transcription (RT)-PCR in cultured hepatocytes after 2.5 h of culture but was significantly detected after 22 h of culture (Fig. 2A), reaching a maximum value after 48 h of culture (Fig. 2B). These results indicate
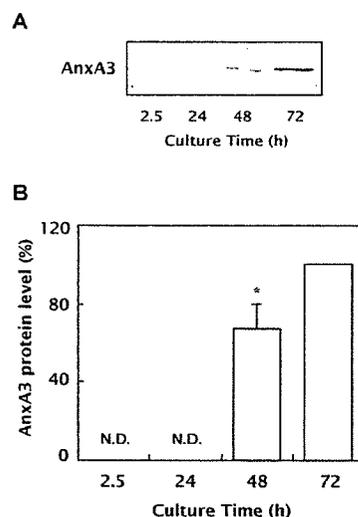

Fig. 1. Expression of AnxA3 Protein during Culture

(A) The data shown are representative of the Western blot analysis results. Cells lysates were prepared from the cells at the indicated times and used for the Western blot analysis. (B) The intensity of each band was quantified, and the results are shown relative to the value of cells cultured for 72 h. The data are expressed as the mean±S.D. of 3 experiments. *$p<0.01$, compared with the value of cells cultured for 72 h. N.D., not detected.
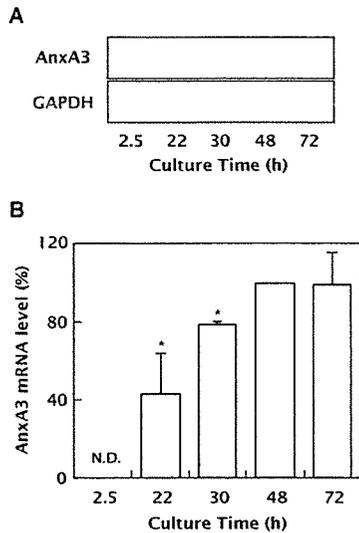
Fig. 2.   Increase in AnxA3 mRNA Level during Culture

(A) The data shown are representative of the RT-PCR analysis results. Total RNA was prepared from the cells at the indicated times and used for the RT-PCR analysis. (B) The intensity of each band was quantified, and the results are shown relative to the value of cells cultured for 48 h. The data are expressed as the mean±S.D. of 3 experiments. *p<0.01, compared with the value of cells cultured for 48 h. N.D., not detected.
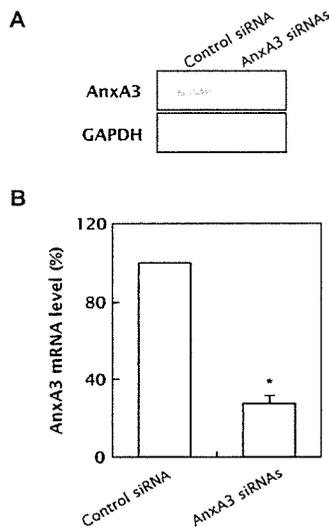

Fig. 3.   Suppression of Increase in AnxA3 mRNA Level during Culture with RNAi

(A) The data shown are representative of the RT-PCR analysis results. Total RNA was prepared from the cells 1 d after siRNA transfection and used for the RT-PCR analysis. (B) The intensity of each band was quantified, and the results are shown relative to the value of cells transfected with control siRNA. The data are expressed as the mean±S.D. of 3 experiments. *p<0.01, compared with the value of cells transfected with control siRNA.

that the expression of AnxA3 is regulated by its mRNA level.

Suppression of AnxA3 Expression Using RNA Interference   Next, we attempted to suppress AnxA3 expression by RNA interference (RNAi) to examine the role of ANXA3 in the cultured hepatocytes. AnxA3 mRNA expression was markedly reduced by treatment with AnxA3 siRNAs, compared with the expression after treatment with control siRNA, 1 d after the transfection (Fig. 3A), with an inhibition of approximately 80% (Fig. 3B). Furthermore, the AnxA3
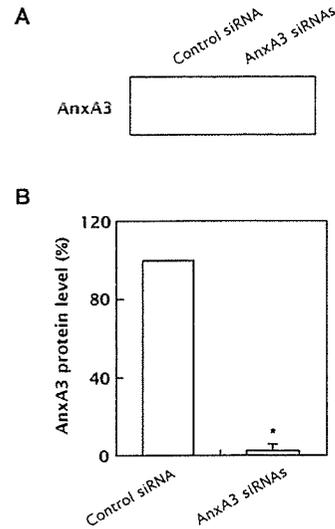

Fig. 4.   Suppression of AnxA3 Protein Expression during Culture with RNAi

(A) The data shown are representative of the Western blot analysis results. Cells lysates were prepared from the cells 1 d after siRNA transfection and used for the Western blot analysis. (B) The intensity of each band was quantified, and the results are shown relative to the value of cells transfected with control siRNA. The data are expressed as the mean±S.D. of 3 experiments. *p<0.01, compared with the value of cells transfected with control siRNA.

protein level was also reduced by the treatment with AnxA3 siRNAs compared with the level after treatment with control siRNA (Fig. 4A), with an inhibition of more than 95% (Fig. 4B). On the other hand, the control siRNA had almost no effect on AnxA3 protein and mRNA levels compared with those treated with SiFector alone (data not shown). Neither the control nor AnxA3 siRNAs caused any cytotoxic effects, as observed microscopically or by the quantification of the total amount of protein in each sample (data not shown). These results indicate that AnxA3 siRNAs efficiently and specifically inhibit the expression of AnxA3 in primary cultured parenchymal rat hepatocytes.

Inhibition of DNA Synthesis by Suppression of AnxA3 Expression Using RNAi   Finally, we examined the role of AnxA3 in DNA synthesis by suppressing AnxA3 expression using RNAi. EGF (2 ng/ml) and HGF (20 ng/ml) stimulated DNA synthesis by approximately 7-fold and 9-fold, respectively in hepatocytes treated with control siRNA (Fig. 5). The stimulations were inhibited to approximately 70% by treatment with AnxA3 siRNAs. Similar results were also obtained in the control cells, whereas the control siRNA had almost no effect on DNA synthesis, compared with the effect in cells treated with SiFector alone (data not shown).

DISCUSSION

In the present study, we showed for the first time that AnxA3 is expressed in cultured parenchymal rat hepatocytes and that the inhibition of AnxA3 expression by RNAi resulted in a significant inhibition of DNA synthesis, suggesting that the expression of AnxA3 is necessary for DNA synthesis in primary cultured parenchymal rat hepatocytes.

Hepatocytes placed under culture conditions, are known to acquire a growth potential characterized by the enhancement of DNA synthesis, which is caused by several growth
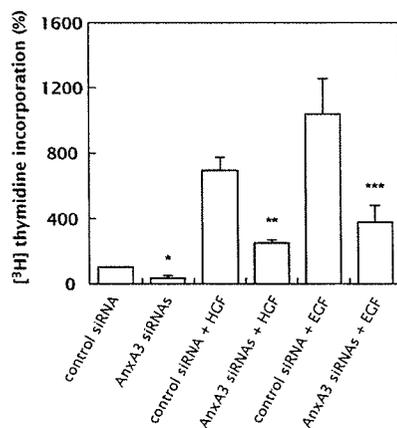
Fig. 5. Inhibition of DNA Synthesis by RNAi

The results are shown relative to the value of control cultured cells transfected with control siRNA. The data are expressed as the mean±S.D. of duplicate wells in 3 experiments. $*p<0.01$, compared with the value of control cultured cells transfected with control siRNA. $**p<0.01$, compared with the value of cells cultured in the presence of HGF and transfected with control siRNA. $***p<0.01$, compared with the value of cells cultured in the presence of EGF and transfected with control siRNA. The mean±S.D. of [^{3}H]thymidine incorporation in the control cultured cells transfected with control siRNA was $9.72\times10^4\pm0.68\times10^4$ dpm/mg protein.

factors.[27,28] Our present findings suggest that the expression of AnxA3 is partly necessary for hepatocytes to acquire a growth potential under culture conditions. In fact, the enhanced expression of AnxA3 has been observed in hepatocellular carcinoma cell lines.[29] In addition, we discovered that the enhanced expression of Anx3 was observed in the proliferative hepatocytes after carbon tetrachloride-induced rat liver damage (unpublished observations).

As for other annexins, several findings concerning the relation of AnxA1 to hepatocyte growth has been reported as described below. The suppression of AnxA1 expression using antisense technology inhibited proliferation in a mouse hepatocyte cell line.[30] AnxA1 increased in the proliferative hepatocytes after carbon tetrachloride-induced rat liver damage or a partial hepatectomy and in hepatocellullar carcinoma tissue.[31,32]

Although the mechanism of action of AnxA3 on DNA synthesis is presently uncertain, the target of AnxA3 may be a common signal transduction pathway, and not necessarily a constitutive or growth factor-mediated one, because the suppression of AnxA3 expression using RNAi not only inhibited the control of DNA synthesis, but also EGF- or HGF-stimulated DNA synthesis, almost to a similar level. In this respect, the findings described below may be relevant to speculations on the mechanism of action of AnxA3 on DNA synthesis. The growth factor-mediated enhancement of hepatocyte growth consists of several signal transduction pathways.[33] The activation of cytosolic phospholipase A_2 (cPLA$_2$) by MAP kinase liberates arachidonic acid from phospholipids and is followed by the generation of prostaglandins, mediators of DNA synthesis, via cyclooxygenase. Interestingly, the suppression of AnxA1 expression using antisense technology inhibited cPLA$_2$ activity in a mouse hepatocyte cell line.[30] This report suggests that cPLA$_2$ must be phosphorylated by AnxA1 to become active. Additional evidence suggests that AnxA1 (275—346 aa), the region responsible for phospholipid binding is necessary for the interaction between AnxA1 and cPLA$_2$.[34] Further study

is required to clarify the mechanism of action of AnxA3, including the possibility that AnxA3 positively modulates cPLA$_2$ activity, as in the case of AnxA1.

REFERENCES

1) Crumpton M. J., Dedman J. R., Nature (London), 345, 212 (1990).
2) Raynal P., Pollard H. B., Biochim. Biophys. Acta, 1197, 63—93 (1994).
3) Gerke V., Moss S. E., Physiol. Rev., 82, 331—371 (2002).
4) Moss S. E., Morgan R. O., Genome Biol., 5, 219. 1—8 (2004).
5) Tait J. F., Sakata M., McMullen B. A., Miao C. H., Funakoshi T., Hendrickson L. E., Fujikawa K., Biochemistry, 27, 6268—6276 (1988).
6) Ernst J. D., Hoye E., Blackwood R. A., Jaye D., J. Clin. Invest., 85, 1065—1071 (1990).
7) Gunteski-Hamblin A. M., Song G., Walsh R. A., Frenzke M., Boivin G. P., Dorn G. W., 2nd, Kaetzel M. A., Horseman N. D., Dedman J. R., Am. J. Physiol., 270, H1091—1100 (1996).
8) Kubista H., Hawkins T. E., Patel D. R., Haigler H. T., Moss S. E., Curr. Biol., 9, 1403—1406 (1999).
9) Srivastava M., Atwater I., Glasman M., Leighton X., Goping G., Caohuy H., Miller G., Pichel J., Westphal H., Mears D., Rojas E., Pollard H. B., Proc. Natl. Acad. Sci. U.S.A., 96, 13783—13788 (1999).
10) Herr C., Smyth N., Ullrich S., Yun F., Sasse P., Hescheler J., Fleischmann B., Lasek K., Brixius K., Schwinger R. H., Fassler R., Schroder R., Noegel A. A., Mol. Cell. Biol., 21, 4119—4128 (2001).
11) Song G., Harding S. E., Duchen M. R., Tunwell R., O'Gara P., Hawkins T. E., Moss S. E., Faseb. J., 16, 622—624 (2002).
12) Roviezzo F., Getting S. J., Paul-Clark M. J., Yona S., Gavins F. N., Perretti M., Hannon R., Croxtall J. D., Buckingham J. C., Flower R. J., J. Physiol. Pharmacol., 53, 541—553 (2002).
13) Hannon R., Croxtall J. D., Getting S. J., Roviezzo F., Yona S., Paul-Clark M. J., Gavins F. N., Perretti M., Morris J. F., Buckingham J. C., Flower R. J., Faseb. J., 17, 253—255 (2003).
14) Croxtall J. D., Gilroy D. W., Solito E., Choudhury Q., Ward B. J., Buckingham J. C., Flower R. J., Biochem. J., 371, 927—935 (2003).
15) Rand J. H., N. Engl. J. Med., 340, 1035—1036 (1999).
16) Niimi S., Hyuga M., Harashima M., Seki T., Ariga T., Kawanishi T., Hayakawa T., Biol. Pharm. Bull., 27, 1864—1868 (2004).
17) Niimi S., Oshizawa T., Yamaguchi T., Harashima M., Seki T., Ariga T., Kawanishi T., Hayakawa T., Biochem. Biophys. Res. Commun., 300, 770—774 (2003).
18) Kaetzel M. A., Hazarika P., Dedman J. R., J. Biol. Chem., 264, 14463—14470 (1989).
19) Comera C., Rothhut B., Cavadore J. C., Vilgrain I., Cochet C., Chambaz E., Russo-Marie F., J. Cell. Biochem., 40, 361—370 (1989).
20) Kristensen B. I., Kristensen P., Johnsen A. H., Int. J. Biochem., 25, 1195—1202 (1993).
21) Pepinsky R. B., Tizard R., Mattaliano R. J., Sinclair L. K., Miller G. T., Browning J. L., Chow E. P., Burne C., Huang K. S., Pratt D., Walchter L., Hession C., Frey A. Z., Wallner B. P., J. Biol. Chem., 263, 10799—10811 (1988).
22) Tanaka K., Sato M., Tomita Y., Ichihara A., J. Biochem. (Tokyo), 84, 937—946 (1978).
23) Romisch J., Schuler E., Bastian B., Burger T., Dunkel F. G., Schwinn A., Hartmann A. A., Paques E. P., Blood Coagul. Fibrinolysis, 3, 11—17 (1992).
24) Uno S., Nakamura M., Seki T., Ariga T., Biochem. Biophys. Res. Commun., 239, 123—128 (1997).
25) Niimi S., Horikawa M., Seki T., Ariga T., Kobayashi T., Hayakawa T., Biol. Pharm. Bull., 25, 437—440 (2002).
26) Bradford M. M., Anal. Biochem., 72, 248—254 (1976).
27) Fausto N., Laird A. D., Webber E. M., Faseb. J., 9, 1527—1536 (1995).
28) Michalopoulos G. K., DeFrances M. C., Science, 276, 60—66 (1997).
29) Liang R. C., Neo J. C., Lo S. L., Tan G. S., Seow T. K., Chung M. C., J. Chromatogr. B Analyt. Technol. Biomed. Life Sci., 771, 303—328 (2002).
30) de Coupade C., Gillet R., Bennoun M., Briand P., Russo-Marie F.,

Solito E., *Hepatology*, **31**, 371—380 (2000).

31) Masaki T., Tokuda M., Fujimura T., Ohnishi M., Tai Y., Miyamoto K., Itano T., Matsui H., Watanabe S., Sogawa K., Yamada T., Konishi R., Nishioka M., Hatase O., *Hepatology*, **20**, 425—435 (1994).

32) Masaki T., Tokuda M., Ohnishi M., Watanabe S., Fujimura T., Miyamoto K., Itano T., Matsui H., Arima K., Shirai M., Maeba T., So-gawa K., Konishi R., Taniguchi K., Hatanaka Y., Hatase O., Nishioka M., *Hepatology*, **24**, 72—81 (1996).

33) Adachi T., Nakashima S., Saji S., Nakamura T., Nozawa Y., *Hepatology*, **21**, 1668—1674 (1995).

34) Kim S. W., Rhee H. J., Ko J., Kim Y. J., Kim H. G., Yang J. M., Choi E. C., Na D. S., *J. Biol. Chem.*, **276**, 15712—15719 (2001).

Full Paper

Simultaneous Real-Time Detection of Initiator- and Effector-Caspase Activation by Double Fluorescence Resonance Energy Transfer Analysis

Hiroshi Kawai[1], Takuo Suzuki[1], Tetsu Kobayashi[1], Haruna Sakurai[2], Hisayuki Ohata[2], Kazuo Honda[2], Kazutaka Momose[2], Iyuki Namekata[3], Hikaru Tanaka[3], Koki Shigenobu[3], Ryu Nakamura[4], Takao Hayakawa[1], and Toru Kawanishi[1,]*

[1]*Division of Biological Chemistry and Biologicals, National Institute of Health Sciences, Tokyo 158-8501, Japan*
[2]*Department of Pharmacology, School of Pharmaceutical Sciences, Showa University, Tokyo 142-8555, Japan*
[3]*Department of Pharmacology, Toho University School of Pharmaceutical Sciences, Chiba 274-8510, Japan*
[4]*Carl Zeiss Co., Ltd., Tokyo 160-0003, Japan*

Abstract. Fluorescence resonance energy transfer (FRET) with green fluorescent protein (GFP) variants has become widely used for biochemical research. In order to expand the choice of fluorescent range in FRET analysis, we designed various color versions of the FRET-based probes for caspase activity, in which the substrate sequence of the caspase was sandwiched by donor and acceptor fluorescent proteins, and studied the potential of these color versions as fluorescent indicators. Six color versions were constructed by a combination of cyan fluorescent protein (CFP), GFP, yellow fluorescent protein (YFP), and DsRed. Real-time monitoring in single cells revealed that all probes could detect caspase activation during tumor necrosis factor (TNF)-α-induced cell death as a fluorescent change. GFP-DsRed and YFP-DsRed were as sensitive as CFP-YFP, and CFP-DsRed also showed a large fluorescent change. By using two probes, CFP-DsRed and YFP-DsRed, we carried out simultaneous multi-FRET analysis and revealed that the initiator- and effector-caspases were activated almost simultaneously in TNF-α-induced cell death. These findings may give experimental bases for the development of novel techniques to analyze multi-events simultaneously in single cells by using FRET probes in combination.

Keywords: fluorescence resonance energy transfer, green fluorescent protein, tumor necrosis factor-α, cell death, caspase

Introduction

Many probes for various physiological reactions have been developed with green fluorescent protein (GFP) variants by using a similar strategy as that used with cameleon, the Ca^{2+}-sensing fusion protein developed by Miyawaki et al. (1 – 9). The cameleon consists of cyan fluorescent protein (CFP), calmodulin, M13 peptide, and yellow fluorescent protein (YFP). This fusion protein senses Ca^{2+} as the change of fluorescence resonance energy transfer (FRET) efficiency between CFP and YFP. Calmodulin binds M13 in the presence of Ca^{2+}, which causes conformational change in cameleon,

resulting in a change in the distance between and relative orientation of CFP and YFP. This change alters the FRET efficiency from CFP to YFP; therefore, Ca^{2+} can be monitored as the fluorescent change (1).

CFP and YFP are the most frequently used pair for analysis by FRET. This pair is suitable for FRET analysis because the spectral overlap between the emission of the donor protein (CFP) and the excitation of the acceptor protein (YFP) is sufficient for energy transfer, and their ranges of fluorescence are far apart enough to be separated by measuring devices such as fluorescent microscopy (10). However, there are limitations for the CFP-YFP pair. It is impossible, for example, to use the CFP-YFP FRET probe for simultaneous measurement with other probes that are made of GFP variants or have

*Corresponding author. FAX: +81-3-3700-9064
E-mail: kawanish@nihs.go.jp.

fluorescein structure. If more choice of FRET probes is available from wider fluorescence ranges, it would allow us to analyze multi-events simultaneously occurring in living cells.

In this paper, we developed caspase-sensors of various colors by using cyan, green, yellow, and red fluorescent proteins and assessed their ability to detect the caspase activation in living single cells. Based on the findings obtained, we tried to perform multi-event FRET analysis and clarify the temporal relationships between biochemical reactions during cell death.

Materials and Methods

Plasmid construction

Plasmid encoding CY-sensor, YFP-peptide-CFP, was generated as previously reported (11). The sequence encoding 11 amino acids at the C-terminus of YFP was eliminated in this construct. The C-terminal truncated forms of the CFP (or GFP) gene were generated by PCR with primers containing the NheI site or BspEI site and pECFP-C1 (or pEGFP-C1; Clontech, Palo Alto, CA, USA) as a template, and the restricted fragment was inserted into the NheI/BspEI sites of the CY-sensor to generate a plasmid carrying truncated CFP (or GFP) at the N-terminus. DsRed was generated from pDsRed2-C1 (Clontech) by PCR, at the AgeI/NotI sites, and the restricted fragment was inserted into the AgeI/NotI sites of the CY-sensor to generate a plasmid carrying DsRed2 at the C-terminus. CG-, CR-, GR-, and YR-sensors were generated with a combination of these elements. The AgeI/BsrGI fragment from pEGFP-C1 was inserted into the AgeI/BsrGI sites of the CY-sensor to generate the GY-sensor. All cloned sequences were verified by sequencing.

Cell culture and transfection

HeLa cells were cultured in DMEM (Sigma-Aldrich, St. Louis, MO, USA) supplemented with 100 units/ml of penicillin G, 100 μg/ml of streptomycin, and 10% fetal calf serum (Invitrogen Corp., Carlsbad, CA, USA). Plasmid encoding the sensor protein was transfected into HeLa cells using Effectene Transfection Reagent (Qiagen, Hilden, Germany) according to the manufacturer's instructions. After 12 – 24 h incubation with the transfection reagent, the cells were washed with PBS and cultivated on dishes suitable for assay in medium containing 500 μg/ml of G418 for an additional 1 – 3 days until the assay was performed.

Western blotting

Cells cultured in a plastic dish were washed with PBS and lysed with 1 × SDS loading buffer. The samples dissolved in 1 × SDS loading buffer were incubated at 95°C for 2 min, and then they were loaded onto SDS-polyacrylamide gels (10%). Proteins were separated at 20 mA and then blotted to PVDF membranes in Tris-glycine transfer buffer at 100 V for 2 h. The membrane was incubated with block ace (Dainippon Pharmaceutical, Osaka) for 1 h, anti-GFP peptide antibody (Clontech, diluted with 0.1 × block ace to 1:1,000) for 2 h, and anti-rabbit IgG horseradish peroxidase-conjugated secondary antibody (Chemicon International Inc., Temecula, CA, USA; diluted with 0.1 × block ace to 1:10,000) for 1 h. The membrane was washed with TBS-T 3 times for 5 min after the incubation with the antibody. All of these incubations were performed at room temperature. The membrane was developed with the ECL chemiluminescence detection reagent (Amersham Biosciences, Piscataway, NJ, USA).

Measurement of fluorescent spectra of the sensors in HeLa cells

Spectral imaging was performed with LSM510META (Carl Zeiss, Jena, Germany) (12). Cells expressing one of the sensors were observed by excitation light at 458 nm (Ar laser), emitted fluorescence was separated by a grating, and the separated fluorescence were detected by 24 photomultiplier tubes (PMT) that were set to detect fluorescence at 468 – 714 nm. Each PMT detected fluorescence in the 10.7-nm wavelength range. So, the fluorescent spectrum at 468 – 714 nm was obtained with 10.7-nm resolution. Cell death was induced by incubation with tumor necrosis factor (TNF)-α (100 ng/ml) and cycloheximide (CHX, 10 μg/ml) for 6 h. Fluorescent spectra of living and dead cells were obtained from the whole cell region of normal-shaped and spherical cells, respectively.

Real-time imaging with FRET sensors

Transfected cells were cultured on a cover glass (25-mm diameter, 0.15 – 0.18-mm thickness) for 1 – 3 days. Cells were treated with TNF-α/CHX and then incubated under the usual culture condition for 1 – 2 h before analysis. Analyses were carried out by confocal laser-scanning fluorescent microscopy using a Carl Zeiss LSM510 system. During the observation, the media were buffered with 10 mM hepes buffer (pH 7.4), and the cells were maintained at 35 – 37°C. DIC images and grayscale images for fluorescence channels were obtained every 2 min unless otherwise described. Excitation lights for the FRET probe (458 nm for the CG-, CY-, GY-, and CR-sensors; 488 nm for the GR- and YR-sensors) were provided by an Ar laser with a 458 or 488 dichroic mirror. Images of the FRET probe were obtained separately for both donor and acceptor

Table 1. Measurement conditions for real-time analysis by LSM510

Sensor	Fusion protein[a]	Excitation (nm)[b]	Emission (nm)[c]		
			beam splitter	emission filter	
				donor	acceptor
CG	GFP-peptide-CFP	458	515	467.5 – 497.5	515 – 545
CY	YFP-peptide-CFP	458	515	467.5 – 497.5	515 – 545
GY	YFP-peptide-GFP	458	515	475 – 525	515 – 545
CR	CFP-peptide-DsRed	458	515	467.5 – 497.5	560 – 615
GR	GFP-peptide-DsRed	488	545	505 – 530	560 – 615
YR	YFP-peptide-DsRed	488	545	505 – 530	560 – 615

[a]N-terminal CFP, GFP, and YFP were in a truncated form in which 11 amino acids at the C-terminus were eliminated, and His₁₀ was present at the C-terminus of CG, CY, and GY. [b]Excitation light was obtained by Ar laser and a 458 or 488 dichroic mirror. [c]Emitted fluorescence was separated by a 515 or 545 dichroic mirror, and the fluorescence of the donor and that of the acceptor were obtained through band pass emission filters.

fluorescence using a dichroic mirror and band-pass emission filters as shown in Table 1. Images were processed and quantified using MetaFluor software as follows: The average pixel intensity of the fluorescence of the whole cell region was determined for each channel. The ratio value was calculated as the average pixel value of the fluorescent ratio, (fluorescent intensity for the acceptor channel) / (fluorescent intensity for the donor channel), in the whole cell region. As cells changed their morphology during the observation, the whole cell region was determined separately in each image.

Results

Construction and characterization of FRET probes

We developed plasmids expressing caspase sensors as shown in Fig. 1a. A 12-amino-acid peptide derived from poly(ADP-ribose)polymerase (PARP) that is a well-known substrate of effector caspases was sandwiched by two different fluorescent proteins (an example of CFP-YFP is shown in Fig. 1a). The peptide sequence contains a caspase recognition site in the middle, and this fusion protein was cleaved mainly by caspase-3 (11). CFP-GFP, CFP-YFP, GFP-YFP, CFP-DsRed, GFP-DsRed, and YFP-DsRed were used as the donor-acceptor pairs. We named these fusion proteins CG-, CY-, GY-, CR-, GR-, and YR-sensor, respectively (Table 1). These fusion proteins show FRET in their intact form, whereas in the presence of active caspase, the peptide sequence is cleaved, CFP and YFP are far apart, and the fusion proteins do not show FRET any longer. The fluorescent ratio of acceptor/donor reflects the amount of FRET, so we used the reduction of this value as an index of caspase activation.

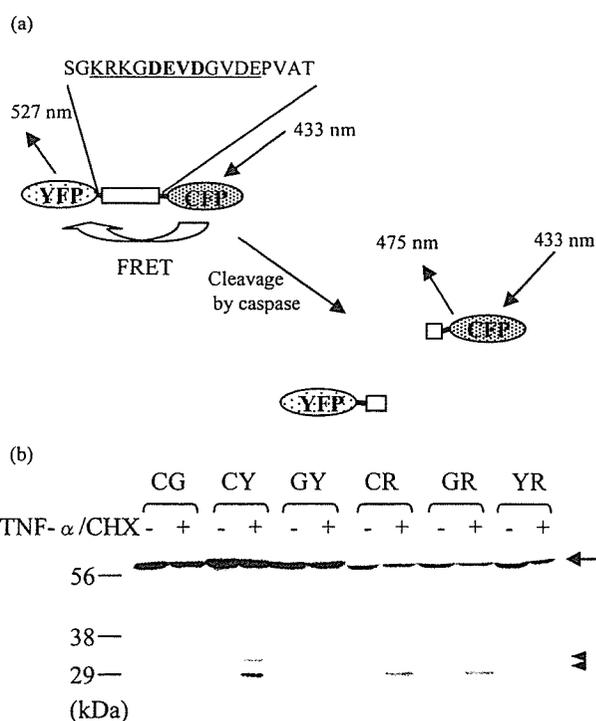HeLa cells expressing one of these fusion proteins

(a)

(b)

Fig. 1. Small peptide sandwiched by two different fluorescent proteins can be a caspase-sensor. a: Fusion protein that consists of a PARP-derived 12-amino-acid peptide sandwiched by CFP and YFP exhibits FRET in its intact form. In the presence of active caspases, the peptide is cleaved, and the fusion protein does not exhibit FRET. Caspase activation can be detected by measuring the fluorescence of CFP and YFP. b: Six caspase-sensors expressed in HeLa cells were cleaved by cell death stimuli. HeLa cells expressing one of the sensors were incubated in the presence or absence of TNF-α/CHX for 6 h. The arrow and arrowhead indicate the full length and cleaved fragments of the sensors.

were treated with TNF-α/CHX. After 6-h exposure, the sensor proteins in cells were extracted and analyzed by western blotting. All 6 fusion proteins were detected in their intact forms in non-treated HeLa cells (arrow in Fig. 1b), and small fragments were detected in cells treated with TNF-α/CHX (arrowhead in Fig. 1b), indicating that the fusion proteins were cleaved by cell death stimuli, as expected. The antibody used in this analysis reacts with CFP, GFP, and YFP, but not with DsRed. Therefore, CG-, CY-, and GY-sensor showed two cleaved fragments corresponding to the N- and C-terminal C/G/YFP, whereas CR-, GR-, and YR-sensor showed only one cleaved fragment corresponding to the N-terminal C/G/YFP.

Figure 2 shows the fluorescent spectra of the probes in living or dead cells. Comparing the fluorescence of living and dead cells, all sensors showed an increase of donor fluorescence and/or a reduction of acceptor fluorescence in response to cell death stimuli. This change results in a reduction of fluorescent ratio of acceptor/donor that is an index of FRET. These sensors were designed to show a reduction of FRET with caspase activation, so these results suggest that all 6 fusion proteins work as expected and can detect caspase activation as fluorescent change in living cells.

For simultaneous application of two or more fluorescent probes, minimum spectral overlap between probes is one of the important conditions. The spectra in Fig. 2 give us a clue to determine a suitable combination of probes for multi-probe analysis. CG-, CY-, or GY-sensor has the least fluorescence in the red-fluorescence

region (>600 nm), so it is possible to use this fluorescent region for another dye. We can use a red-fluorescent dye that has fluorescence in this region together with CG-, CY-, or GY-sensor simultaneously. On the other hand, YR-sensor has the least fluorescence in the blue-cyan region (<500 nm), so blue-cyan-fluorescent dye is applicable with this probe for the purpose of simultaneous fluorescence imaging. The color variations of FRET probe may be useful for multi-probe analysis.

Real-time detection of caspase activation in living cells

Next, we applied the sensor proteins to real-time measurement. HeLa cells expressing one of the sensor proteins were analyzed with a time resolution of 2 min by laser-scanning confocal fluorescent microscopy. Figure 3 shows typical images (a) and fluorescent changes (b) during cell death. HeLa cells expressing GR-sensor were treated with TNF-α/CHX. An increase of donor protein fluorescence (GFP), a reduction of acceptor protein fluorescence (DsRed), and a reduction of the fluorescent ratio of acceptor/donor (DsRed/GFP) were observed in each cell at a different time. Caspases began to work at the point when the fluorescent ratio began to decrease.

All sensors showed similar changes, meaning that all sensors were useful for real-time detection of the caspase activation in a living cell, although the apparent sensitivity was different between sensors. In order to compare the sensitivity of these sensors to detect the caspase activation, the amount of the fluorescent change was calculated. We defined the start point and the end
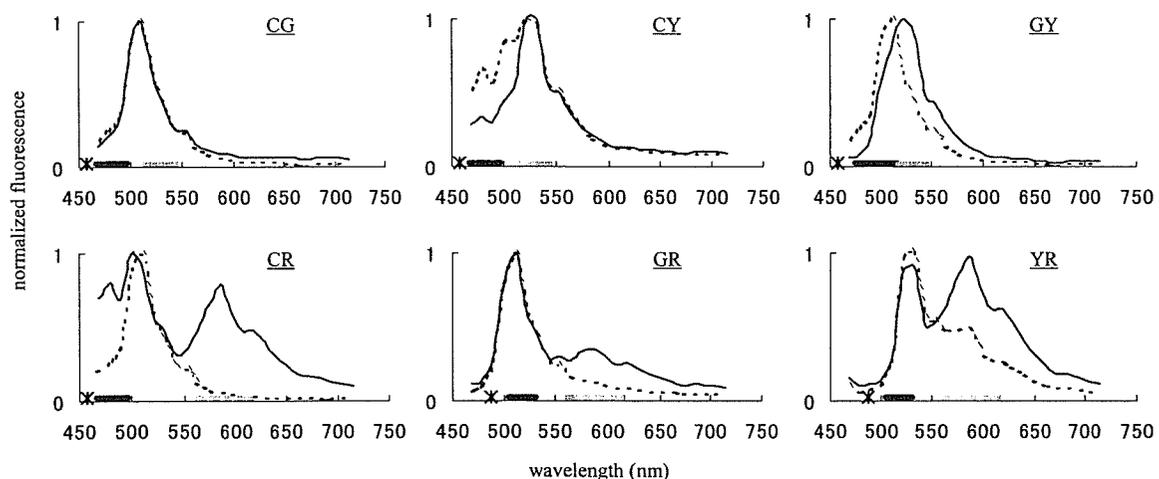

Fig. 2. Fluorescent spectra of the caspase-sensors in HeLa cells. HeLa cells expressing each sensor were treated with TNF-α/CHX for 6 h. The spectra of living cells (solid line) and dead cells (dotted line) were obtained from normal-shaped and spherical cells, respectively. Each spectrum was normalized to the peak that showed maximal intensity. The asterisks and bars on horizontal axes represent the excitation wavelength and detection range for the emitted fluorescence, respectively, used in real-time imaging analysis. Each spectrum is the average of data from 13 – 26 cells.